frontiers | Frontiers in Ecology and Evolution

TYPE Original Research
PUBLISHED 05 October 2022
DOI 10.3389/fevo.2022.942968

OPEN ACCESS

EDITED BY
Jason Newton,
University of Glasgow, United Kingdom

REVIEWED BY
W. Ryan James,
Florida International University,
United States
Vincent Raoult,
The University of Newcastle, Australia

*CORRESPONDENCE
Alex S. J. Wyatt
wyatt@ust.hk

SPECIALTY SECTION
This article was submitted to
Population, Community,
and Ecosystem Dynamics,
a section of the journal
Frontiers in Ecology and Evolution

RECEIVED 13 May 2022
ACCEPTED 22 August 2022
PUBLISHED 05 October 2022

CITATION
Skinner C, Pei Y-D, Morimoto N,
Miyajima T and Wyatt ASJ (2022)
Stable isotopes elucidate body-size
and seasonal fluctuations
in the feeding strategies
of planktivorous fishes across
a semi-enclosed tropical embayment.
Front. Ecol. Evol. 10:942968.
doi: 10.3389/fevo.2022.942968

Stable isotopes elucidate body-size and seasonal fluctuations in the feeding strategies of planktivorous fishes across a semi-enclosed tropical embayment

Christina Skinner[1], Yu-De Pei[1], Naoko Morimoto[2], Toshihiro Miyajima[2] and Alex S. J. Wyatt[1,3]*

[1]Department of Ocean Science, The Hong Kong University of Science and Technology, Kowloon, Hong Kong SAR, China, [2]Department of Chemical Oceanography, Atmosphere and Ocean Research Institute, The University of Tokyo, Kashiwa, Japan, [3]Southern Marine Science and Engineering Guangdong Laboratory (Guangzhou), Guangzhou, China

Reef fish may switch feeding strategies due to fluctuations in resource availability or through ontogeny. A number of studies have explored these trophodynamics using carbon ($\delta^{13}C$) and nitrogen ($\delta^{15}N$) stable isotopes, but additional tracers such as sulfur isotopes ($\delta^{34}S$) show strong potential in systems, where $\delta^{13}C$ and $\delta^{15}N$ results are ambiguous. We tested the utility of adding $\delta^{34}S$ to conventional $\delta^{13}C$ and $\delta^{15}N$ analysis to detect seasonal and body size changes in resource use of two planktivorous damselfish, *Dascyllus reticulatus* and *Dascyllus trimaculatus* across the Puerto Galera embayment in the Philippines. We analyzed stable isotope ratios ($\delta^{13}C$, $\delta^{15}N$, and $\delta^{34}S$) in multiple fish tissues (liver, eye, and muscle) to represent different dietary time frames. We then compared fish tissue isotopes against particulate organic matter (POM) ($\delta^{13}C$ and $\delta^{15}N$) and POM suspension feeder (the tunicate *Polycarpa aurata*: $\delta^{13}C$, $\delta^{15}N$, and $\delta^{34}S$) across the same sites. There were size-based and seasonal differences in damselfish resource use, the latter of which was most pronounced in the fast-turnover liver. Small fish (<70 mm) demonstrated significant seasonality, appearing to switch their resource use between the rainy season and the dry season, while there was no seasonal variation in larger fish (>70 mm). This suggests that smaller fish across the embayment employ an opportunistic feeding strategy to take advantage of fluctuating resource availability, while larger fish exhibits more consistent resource use. Isotope ratios of tunicates and POM further confirmed strong seasonality in this system and a lack of a spatial isotopic gradient. $\delta^{15}N$ did not seem to contribute to consumer resource use patterns, while by contrast,

$\delta^{34}S$ fluctuated significantly between sampling periods and was crucial for demonstrating seasonality in resource use. We recommend including $\delta^{34}S$ when attempting to disentangle seasonal differences in resource use in aquatic food webs using stable isotopes.

KEYWORDS

damselfish, *Dascyllus trimaculatus*, *Dascyllus reticulatus*, multi-tissue analysis, sulfur isotope, carbon isotope, nitrogen isotope

Introduction

Coral reefs are exceptionally complex ecosystems with many internal and external resources available to the many consumers that they host (Hoegh-Guldberg and Dove, 2008). Due to the dynamic nature of these systems, resources fluctuate not only spatially, e.g., across environmental gradients of oceanic exposure (Wyatt et al., 2012b; Page et al., 2013; Zgliczynski et al., 2019), but also temporally, i.e., annually or across distinct seasons (Haas et al., 2010; Erler et al., 2019). Reef fish consumers may therefore alter their resource use according to what is available (Carreón-Palau et al., 2013; Fey et al., 2021), which affects the flow of energy across the entire coral reef food web. To date, seasonality in energy flows and consumer resource use on coral reefs has been poorly studied, with the majority of reef food web studies conducted over limited temporal windows (e.g., Thibodeau et al., 2013; Letourneur et al., 2017; Miller et al., 2019), despite the impact, this may have on the capacity to elucidate key trophodynamic processes (Skinner et al., in press).

In addition to temporal variation in consumer resource use from fluctuations in available material, organisms may change their resource use with ontogeny; as they grow larger they can access larger prey and/or take advantage of previously inaccessible resources (Layman et al., 2005; Cummings et al., 2010; Greenwood et al., 2010). Accessing different resources through ontogeny may provide populations with a degree of resilience to fluctuations in resource availability (Nakazawa, 2015), but there are also implications for the structure of the food web, i.e., as consumer resource use changes, so too does the energy transfer across subsequent trophic levels. Although the presence (or indeed absence) of body size-related changes in resource use is fairly well-documented in coral reef fish (Cocheret de la Morinière et al., 2003; Nakamura et al., 2008; O'Farrell et al., 2014; Plass-Johnson et al., 2015; Matley et al., 2017), interactions between body size and seasonality in resources are seldom considered. For example, do consumers from different size groups respond similarly to temporally fluctuating resources despite taxonomic, and apparent trophic grouping, similarities? Seasonality in basal resources and their use by higher trophic level consumers is highly evident in other equally dynamic systems such as embayments with seagrass beds (Morimoto et al., 2017) and temperate estuaries (Cobain et al., 2022), suggesting that more research into the intricacies of these dynamics on coral reefs is sorely needed.

Stable isotope analysis (SIA) is a useful tool for tracking energy flows and resource use across distinct trophic levels of a food web (Peterson and Fry, 1987; Boecklen et al., 2011). Rather than providing a snapshot view, such as those from traditional techniques, e.g., feeding observations and gut contents analyses, isotope ratios in consumer tissues represent material that has been ingested and assimilated over time, with different tissues representing different dietary time frames based on their rate of isotopic turnover (Tieszen et al., 1983). For example, muscle is a "slow" turnover tissue representing consumer diet over several months, while the liver is a "fast" turnover tissue, representing consumer diet over several weeks (Vander Zanden et al., 2015). While muscle is frequently used in SIA studies of coral reef systems, liver tissue is less often utilised (Skinner et al., in press; but see Roy et al., 2012; Davis et al., 2015; Matley et al., 2016). Studies are also beginning to perform SIA on fish eye lenses, as they have metabolically inert bands (laminae), which are successively deposited throughout their life span, allowing reconstruction of an individual's trophic history (Wallace et al., 2014; Bell-Tilcock et al., 2021). However, successfully dissecting and analyzing distinct bands of a fish's eye lens is time consuming, particularly for smaller species. Few studies have employed SIA of the whole eye (i.e., including the iris, cornea, and retina) despite it being a comparatively easier preparation. Although measuring stable isotope ratios across multiple consumer tissues can provide important information about the temporal dynamics of resource use, ~70% of coral reef food web SIA studies focus solely on a single tissue type (Skinner et al., in press). Furthermore, while studies regularly employ carbon ($\delta^{13}C$) and nitrogen ($\delta^{15}N$) stable isotopes to understand food web energy flows, sulfur ($\delta^{34}S$) is increasingly being used as a third tracer to disentangle sources in aquatic systems, as it can help determine the importance of benthic vs. pelagic inputs (Connolly et al., 2004; McCauley et al., 2014; Skinner et al., 2019b), and there is minimal fractionation across trophic levels

(Barnes and Jennings, 2007). As such, it may represent a highly useful tool for identifying seasonality in aquatic food webs.

To better understand seasonal fluctuations in reef food web dynamics, we set out to determine how the resource use of two damselfish (*Dascyllus reticulatus* and *Dascyllus trimaculatus*) varied seasonally and with body size across a semi-enclosed embayment in the Philippines, where primary production varies seasonally (San Diego-McGlone et al., 1995). These two species are well suited to investigate reef resource dynamics as follows: (1) they are known planktivores with a well-documented diet, and thought to play an important role in capturing available suspended material which then becomes available to higher trophic levels, (2) they are relatively site-attached so their isotope ratios represent the location at which they are caught, and (3) there are size-based behavioral differences in their habitat use as juveniles remain closely attached to small coral heads, while larger individuals exploit a large spatial area (Allen, 1991; Frédérich et al., 2009, 2016; Zikova et al., 2011; Wyatt et al., 2012a; Gajdzik et al., 2016). To further maximize the dietary information obtained from each individual, multiple tissue types assumed to have distinctly varying isotopic turnover rates were sampled (liver, whole eye, and muscle). Specifically, we asked: (1) does damselfish resource use vary seasonally and/or with body size? (2) Are patterns related to fluxes of available material and/or are they represented in the isotope ratios of other consumers of suspended material? and (3) How insightful is the addition of $\delta^{34}S$ as a tracer for exploring these food web dynamics?

Materials and methods

Study site

This study focused on five main sampling sites across the semi-enclosed embayment at Puerto Galera, Philippines (13.515°N, 120.96°E). Sites were chosen to represent the full range of hydrodynamic conditions across the embayment: they were located in two channels where water enters and exits the bay according to strong tidal currents, Manila Channel (MA) and Batangas Channel (BA), at an intermediary site (MB), and in the sheltered inner bay in the port of Muelle (MU) (**Figure 1**). An additional site outside the enclosed bay was established in Sabang (SA). The close proximity of the sites ensured that latitudinally driven differences in $\delta^{13}C$ values (e.g., Rau et al., 1982) would not confound the interpretation of the sample isotope values. Sampling was conducted during both the dry (monthly average rainfall March: ~58 mm; March 2013: ~19 mm) and the rainy seasons (monthly average rainfall September: ~206 mm; September 2012: ~305; September 2014: ~219 mm) (World Weather Online, 2022). Water temperature in the dry season (March 2013) was 26.0 ± 0.3°C, while in the rainy season, it was 28.3 ± 0.6°C (September 2012) and 28.5 ± 0.5°C (September 2014). Available primary production (evidenced by levels of chlorophyll *a*) is higher during the dry season (March 2013: 0.39 ± 0.30 ppb; September 2012: 0.31 ± 0.18 ppb; Morimoto et al., unpublished data), while terrestrial run-off and levels of nitrate are higher during the rainy season (March 2013: 0.37 ± 0.30 μM; September 2012: 0.48 ± 0.51 μM; Morimoto et al., unpublished data; San Diego-McGlone et al., 1995).

Sample collection

Two species of planktivorous damselfish, the reticulate (*D. reticulatus*, $n = 30$) and the threespot dascyllus (*D. trimaculatus*, $n = 25$), were collected opportunistically at the five sites across the embayment by a SCUBA diver using either clove oil (smaller specimens) or a hand pole spear (larger specimens) in September 2012 (rainy season) and March 2013 (dry season). Additional *D. trimaculatus* ($n = 4$) were collected in October 2014 (rainy season). Both *D. reticulatus* and *D. trimaculatus* feed opportunistically on zooplankton, with smaller individuals predominantly occupying coral colonies, while larger individuals spend more time in the water column (Allen, 1991; Zikova et al., 2011; Frédérich et al., 2016; Gajdzik et al., 2016). To explore size-based changes in resource use, individuals were split into small (<70 mm) and large (>70 mm) size groups based on the size at maturity of other closely related *Dascyllus* species (*Dascyllus albisella*) (Booth, 1995).

To better characterize the available planktonic resources and energy pathways, particulate organic matter (POM) and a suspension feeding consumer (gold-mouth sea squirts, *Polycarpa aurata*, hereafter "tunicates") were also collected across the embayment. As POM baselines are inherently variable and difficult to characterize, tunicates may represent a time-integrated proxy for this pathway (Richoux and Froneman, 2009; Stowasser et al., 2012; Ménard et al., 2014). Tunicates were collected by the diver by hand (dry season $n = 19$; rainy season $n = 29$) to represent suspension feeders. Samples were stored and transported frozen (−20°C) until analysis. POM samples (dry season $n = 15$; rainy season $n = 20$) were collected (0–15 m) using a 10-L Van Dorn Sampler (Rigo) (**Supplementary Figures 1, 2**). The collected water was immediately placed into acid-washed 10-L high-density polyethylene (HDPE) collapsible containers, which were filtered onto pre-combusted 47-mm GF/F filters (0.7 μm) within 6 h of collection prior to freezing (−20°C). The volume of water filtered through each GF/F was recorded based on the change in weight of the HDPE containers.

Voucher specimens of *D. reticulatus* (CECAM-AORI-AW003 and CECAM-AORI-AW007), *D. trimaculatus*

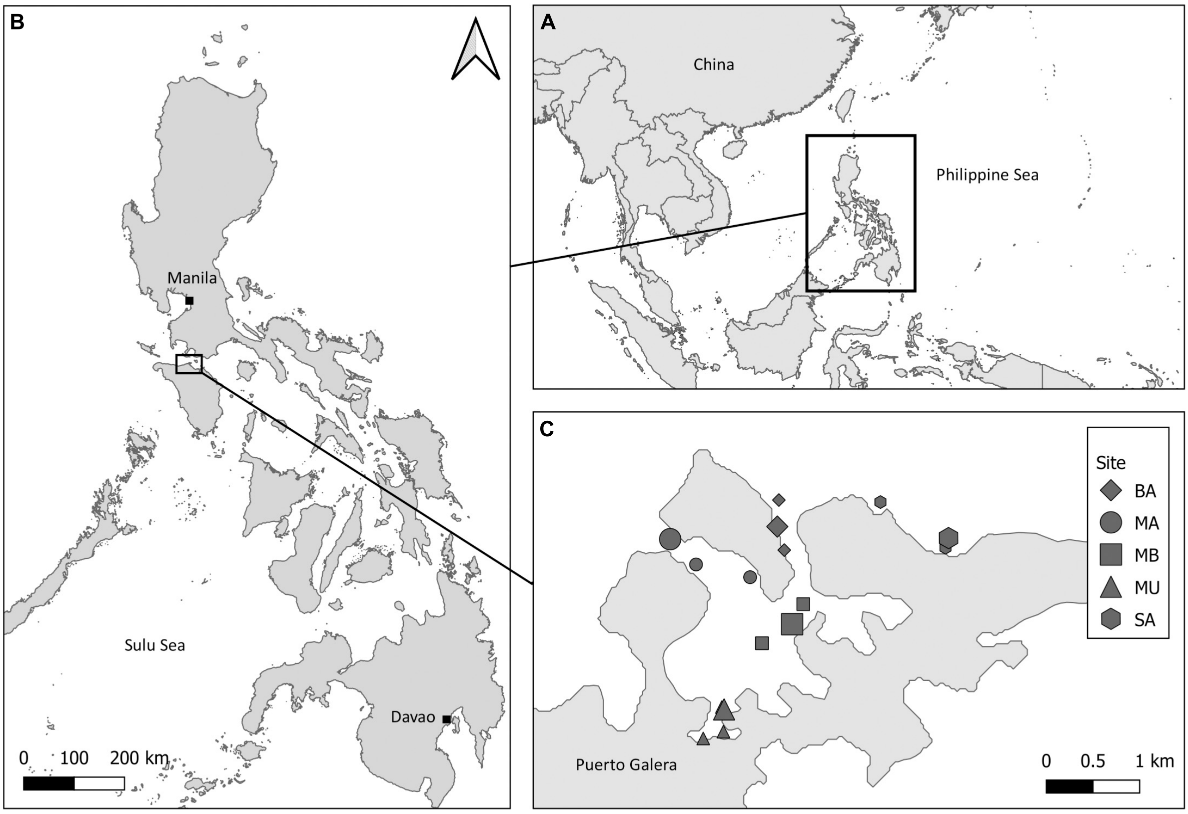

FIGURE 1
(A) Map of the world showing the location of **(B)** Philippines (12.8797° N, 121.7740° E) with **(C)** an inset showing the benthic sampling sites (large symbols: damselfish and tunicates) across the Puerto Galera embayment (13.515° N, 120.96° E). POM sampling locations are linked to nearby benthic sites (small black symbols and same shapes).

(CECAM-AORI-AW004), and *P. aurata* (CECAM-AORI-AW002 and CECAM-AORI-AW006) were deposited with the University of the Philippines' Marine Science Institute.

Sample processing and stable isotope analyses

Fish and tunicates were first thoroughly rinsed with deionized water to reduce the chances of contamination. Length and weight were measured for each *D. reticulatus* and *D. trimaculatus* before dissection of the liver, eye, and white muscle tissues. Total length (cm), the linear dimension between the tip of the snout and the end of the caudal fin, was measured using a Vernier caliper to the nearest millimeter. Weight (g) was measured with an analytical balance (PM400, Mettler Toledo, Columbus, OH, United States) to the nearest 0.1 g. The liver, eye, and white muscle tissues between the pectoral fin and caudal fin were carefully dissected from each specimen for SIA. For *P. aurata*, the incurrent and excurrent siphon tissues with the tunic attached were dissected as they were considered metabolically active (from constantly moving), and care was taken to avoid the inclusion of visceral organs, which may have different stable isotope signatures. All tissue samples were immediately transferred to individual 2 ml Eppendorf tubes after dissection, stored at −20°C, lyophilized (FreeZone 4.5 Liter Freeze Dryer, Labconco, United States) for 72 h, and ground to powder using a ball mill (Beads crusher μT-12, Taitec Ltd., Koshigaya, Saitama, Japan). Approximately ~1.5 mg of ground samples of all tissue types were weighed into 5 × 9 mm tin capsules (Säntis Analytical, Teufen, Switzerland) on a microbalance (MC5, Sartorius, Göttingen, Germany). Where possible, if sufficient material was available, all samples were prepared in duplicate.

Particulate organic matter filters were freeze-dried and then fumigated with concentrated HCl for 48 h to remove inorganic carbonates. After fumigation, they were stored in a vacuum desiccator with several pellets of NaOH for ca. 1 week to remove excess acid. A half piece of each 47-mm filter sample was wrapped with a 10 × 9 mm silver capsule and a 10 × 9 mm tin capsule (Säntis Analytical, Teufen, Switzerland), and then pressed into a tablet using a hand-press tablet maker (internal diameter = 9 mm). The silver capsule was used to remove excess halogens that were normally contained in filter samples and could poison catalysts in the Elemental Analyzer (EA). Combusted GF/F filters retain a small amount of carbon even after pre-combustion, so carbon content (calculated based on the filter C mass and the volume filtered, giving in μg C L^{-1}) and isotope ratios were blank-corrected based on analysis of a few unused filters that were acid-treated in a similar way as the sample filters.

Samples were analyzed for stable carbon, nitrogen, and sulfur in an EA IsoLink system (Thermo Fisher Scientific, Bremen, Germany) coupled with a Delta V Advantage isotope ratio mass spectrometer (IRMS) (Thermo Fisher Scientific, Bremen, Germany). Stable isotope ratios for δ^{15}N, δ^{13}C, and δ^{34}S are reported in delta notation (δ) which is: $[R_{Sample}/R_{Standard}-1]$, where R is the ratio of heavy-to-light isotopes and values are expressed in units of per mil (‰). Certified international reference materials were analyzed every six samples in all runs to correct the isotope values. Reference materials used for δ^{13}C and δ^{15}N were USGS40 (glutamic acid) and USGS-41A (glutamic acid enriched in ^{13}C and ^{15}N). Silver sulfide standards IAEA-S1 and IAEA-S2 were used for δ^{34}S correction. Internal reference material USGS-42 (Tibetan human hair powder) was placed in every ten samples for quality control and drift correction. Analytical precision across all reference materials was: $\delta^{13}C \leq 0.28$; $\delta^{15}N \leq 0.21$; and $\delta^{34}S \leq 0.84$. Two randomly spaced study-specific reference materials were also regularly analyzed to capture analytical variation: muscle tissue of *Salmo salar* and *Xiphias gladius* (analytical precision: $\delta^{13}C \leq 0.28$; $\delta^{15}N \leq 0.19$; and $\delta^{34}S \leq 1.2$; $n = 53$) (**Supplementary Table 1**).

Note that no δ^{34}S data are available for POM. While δ^{34}S analysis was not available for these samples, in addition, determination of δ^{34}S from POM (i.e., GF/F samples) can be technically difficult due to the contamination of seawater sulfate. The concentration of $SO4^{2-}$ in seawater is much higher (ca. 28 mM) than dissolved inorganic carbon (ca. 2 mM), and $SO4^{2-}$ is much more difficult than inorganic carbon to remove from samples without interference with organic carbon and total nitrogen analyses. As such, δ^{34}S could not have been determined accurately for POM, even if δ^{34}S analysis had been available. In addition, the δ^{34}S of phytoplankton is rarely measured directly, but often inferred from the δ^{34}S of organic-S in sinking particles or surface oxic sediment, or just assumed to be very similar to seawater sulfate (ca. +22‰) (cf. Trust and Fry, 1992).

Data analysis

Fish tissues with high lipid content can have biased δ^{13}C values due to the fractionation of carbon during lipid synthesis. If C:N ratios are >3.5, it is recommended that δ^{13}C values are corrected for lipid content (Sweeting et al., 2006; Post et al., 2007; Skinner et al., 2016). All fish tissues had a C:N ratio >3.5 (mean ± SD: liver 7.25 ± 2.66; eye 6.08 ± 1.65; and muscle 4.47 ± 1.17), so δ^{13}C values were mathematically corrected using a lipid normalization model following (Kiljunen et al., 2006), which changed δ^{13}C (mean ± SD) by 3.01 ± 1.35‰ (liver), 2.38 ± 0.93‰ (eye), and 1.4 ± 0.69‰ (muscle). This model is particularly appropriate for the correction of liver tissue as it accounts for non-linear relationships between δ^{13}C and C:N ratios as lipid content increases. High lipid levels in liver tissue may also influence δ^{34}S values: shark liver tissue δ^{34}S decreased by 4.6 ± 0.9‰ after chemical lipid extraction, but there was a minimal influence on muscle or fin tissue (Riverón et al., 2022). To account for the possible influence of high lipid levels on δ^{34}S, damselfish liver δ^{34}S values were also corrected (−4.6‰). However, given the uncertainty in applying this correction factor to planktivorous reef fish, raw liver δ^{34}S values were used in all analyses in the main text, while lipid-corrected δ^{34}S analyses are reported in the **Supplementary material**. Lipid removal is not required for tunicate tissues as despite high C:N ratios (mean ± SD, 7.18 ± 1.09), they have low amounts of lipids (Hagen, 1988; Pakhomov et al., 2019). Similarly, unless nutrients are highly limited (leading to increased lipid storage and reduced growth; Mayzaud et al., 1989; Mock and Gradinger, 2000), pelagic POM lipid levels are low, and removal is not required (Søreide et al., 2006).

Since only the large (>70 mm) *D. trimaculatus* were collected in two separate rainy seasons (2012 and 2014), mixed-effects models were used to determine whether we could pool samples from each rainy season into one group. Using the R package *lme4* v 1.1-26 (Bates et al., 2015), a model was run for each isotope (δ^{13}C, δ^{15}N, or δ^{34}S as the response variable), with year, site, and their interaction as fixed effects, and tissue type (i.e., liver, eye, or muscle) as a random effect (random intercept). ANOVA determined whether the fixed effects were significant or not. While δ^{15}N varied significantly among sites overall, and δ^{34}S varied significantly between years overall, none of the isotopes varied significantly when considering the interaction between Year × Site, indicating no temporal differences at the site level. As such, for each site, large *D. trimaculatus* samples from 2012 to 2014 were pooled (**Supplementary Table 2**).

To explore changes in resource use across different size ranges, rather than separating samples by species, we grouped fish samples into small (<70 mm) and large (>70 mm) size groups. However, first, we used mixed-effects models (R package lme4 v. 1.1-26; Bates et al., 2015) to see whether there was a significant difference in isotope ratios between species within each size group. A model was run for each isotope (δ^{13}C, δ^{15}N, or δ^{34}S as the response variable), species as a fixed effect, and site, season, and tissue as random effects. There were no significant differences in δ^{13}C, δ^{15}N, or δ^{34}S between species for the small size group, so samples from both species were pooled into one "Small" group. For the large size group, there were no significant differences in δ^{13}C or δ^{34}S between species, but there was a marginally significant difference in δ^{15}N ($p = 0.04$). Upon inspection, the large group contained only one individual *D. reticulatus*, and its δ^{15}N values were within the ranges of those of the *D. trimaculatus*, so all large samples were considered as one "Large" group (**Supplementary Table 3**). Consequently, for all remaining analyses, damselfish were considered as either small (<70 mm) or large (>70 mm) and sampled during the dry (March) or rainy (September) season.

Size and seasonal effects on isotope ratios in fish tissues

Length–weight and length–isotope relationships were initially explored for all fish across the embayment using regression analysis. Length–weight relationships were assessed using an exponential regression model with length (mm) as the response variable and log (weight) (g) as the predictor variable. To explore relationships between fish length (mm) and isotope ratios, and how this varied between seasons, a linear regression was used for each tissue, with the isotope ($\delta^{13}C$, $\delta^{15}N$, or $\delta^{34}S$) as the response variable and fish length (mm) and the interaction between fish length and season (dry/rainy) as predictor variables. ANOVA determined whether the fixed effects were significant or not. Where there was no significant effect of the interaction between fish length and season, the regression was rerun with only fish length (mm) as the predictor variable and all fish were pooled.

Different tissue types will vary in their natural isotopic discrimination making direct comparisons of seasonal effects among tissues problematic. To validate possible discrimination effects, we first adjusted tissues for tissue-dependent fractionation (Δ). In teleost fish, mean $\Delta^{13}C$ in the liver is 1.1‰ lower than in muscle, and mean $\Delta^{15}N$ is 0.9‰ lower (Canseco et al., 2022). For fish eye tissue, there is a 1:1 relationship with muscle $\delta^{13}C$, while $\delta^{15}N$ of eye tissue is ~2‰ lower (Kanaya et al., 2019). However, isotopic differences between eye lens and muscle protein ($\Delta^{13}C$ and $\Delta^{15}N$) are <1‰, so likely obscured by analytical error (Quaeck-Davies et al., 2018). Finally, $\Delta^{34}S$ is minimal in teleost fish (Barnes and Jennings, 2007; Bell-Tilcock et al., 2021). As such, for all further analyses, we corrected liver tissue $\delta^{13}C$ and $\delta^{15}N$ by +1.1 and +0.9‰, respectively, but no correction factor was applied to eye $\delta^{13}C$ and $\delta^{15}N$, or to any $\delta^{34}S$ values.

To determine whether resource use varied between fish size groups and seasons across the three tissue types, we first examined each isotope individually (univariate), and then all three isotopes together (multivariate). For the univariate analyses, we ran mixed-effects models with a Bayesian framework in the R package *MCMCglmm* (Hadfield, 2010). By using a Bayesian framework, these models control for heterogeneity in variances and sample sizes and provide a mean estimate with 95% credible intervals for each parameter. For each tissue type (liver, eye, and muscle), we ran a separate model for each isotope ($\delta^{13}C$, $\delta^{15}N$, or $\delta^{34}S$). For $\delta^{13}C$, models were also run with raw (uncorrected) $\delta^{13}C$ values to assess the effect of the lipid correction on the results, while for liver $\delta^{34}S$, models were also run with the lipid-corrected values. Fixed effects were size (small/large), season (dry/rainy), and their interaction, while site was included as a random effect (random intercept). Models were run with Gaussian error distributions and informative priors (V = 1 as an inverse gamma distribution and a low degree of belief nu = 2 for more sampling space). For liver and eye, models were run with 4,000,000 iterations, a burn-in of 3,000,000, and a thinning interval of 300. Due to convergence issues, models were run with 6,000,000 iterations, a burn-in of 4,500,000, and a thin of 400, for muscle tissue. For each model, autocorrelation and convergence were assessed by checking the model trace plots and Geweke diagnostic to ensure less than 5% of the variables were outside the 95% CI.

To further explore fish resource use when considering all three isotopes, we used a principal component analysis (PCA) using the R package *FactoMineR* v.2.4 (Lê et al., 2008). This method visualizes patterns in the dataset with the PCA loadings providing a statistical estimate of the variables driving separation between the groups. Finally, to test the seasonal and tissue-specific differences in multivariate isotope ratios, we ran a Euclidean Permanova with 9,999 permutations for each fish size group using the R package vegan v2.5-7 (Oksanen et al., 2020). To explore how high lipid content in liver tissue might confound results when considering all three isotopes, we also ran the PCA and PERMANOVA using the lipid-corrected liver $\delta^{34}S$ values.

Suspension feeders and resource availability

For the tunicates ($\delta^{13}C$, $\delta^{15}N$, and $\delta^{34}S$) and POM ($\delta^{13}C$, $\delta^{15}N$) isotope ratios and the particulate organic carbon (POC) (μg/L) and particulate organic nitrogen (PON) (μg/L) sampled across the embayment in both seasons, a two-way ANOVA was carried out for each group to determine whether the isotope ratios or concentrations varied spatially or seasonally, with the isotope as the response variable, and season, site, and their interaction as factors. Tukey's honestly significant difference (HSD) test for multiple comparisons was used to identify significant differences between groups. The Shapiro–Wilk and Levene's tests were used to confirm that data conformed to normality and homoscedasticity of variances, respectively.

For all models, model normality and homogeneity assumptions were checked by plotting model residuals. All statistical analyses were conducted in R Statistical Software 4.1.0 (R Core Team, 2021) and RStudio v. 1.4.1717 (R Studio Team, 2020).

Results

A total of 33 small (<70 mm) and nine large (>70 mm) damselfish were sampled in the dry season (March 2013), and nine small and nine large damselfish were sampled in the rainy season (September 2012 and 2014) across the embayment (Figure 2; Supplementary Tables 4, 5). Total ranges in isotope ratios across fish tissues were always narrower in the rainy season. In the dry season, fish δ^{13}C ranged across ~4.4‰ (−19.7 large liver to −15.3 small muscle), while in the rainy season, δ^{13}C ranged across ~4.1‰ (−19.4 large liver to −15.3 large muscle). For δ^{15}N, dry season values ranged across ~4.5‰ (6.0 small liver to 10.4 large muscle), while in the rainy season, δ^{15}N ranged across ~4.1‰ (6.5 small eye to 10.6 large muscle). Finally, dry season δ^{34}S ranged across ~5.3‰ (19.5 small eye and large muscle to 24.75 small liver) but rainy season δ^{34}S ranged across ~4.9‰ (18.4 small muscle to 23.25 large liver) (Figure 2).

Size and seasonal effects on isotope ratios in fish tissues

The exponential relationship between fish length (mm) and body weight (g) was highly significant ($R^2 = 0.97$, $F_{1,52} = 1732$, $p \leq 0.001$; Figure 3A). For the isotope ratios, a significant positive relationship with fish length (mm) was found for eye δ^{13}C ($R^2 = 0.48$, $F_{1,56} = 52.2$, $p \leq 0.001$; Figure 3B) but a weak negative relationship with liver δ^{34}S ($R^2 = 0.11$, $F_{1,54} = 6.9$, $p = 0.01$; Figure 3D). In some cases, there was a significant interaction of fish length with season, so regression analyses were run for each season separately. For both eye and muscle δ^{15}N, there were highly significant positive relationships with fish length in both the dry (eye: $R^2 = 0.70$, $F_{1,39} = 91.02$, $p \leq 0.001$; muscle: $R^2 = 0.38$, $F_{1,40} = 24.12$, $p \leq 0.001$) and the rainy season (eye: $R^2 = 0.81$, $F_{1,15} = 62.26$, $p \leq 0.001$; muscle: $R^2 = 0.74$, $F_{1,14} = 40.71$, $p \leq 0.001$) (Figure 3C). However, for muscle δ^{13}C, relationships with fish length were significant in the dry ($R^2 = 0.71$, $F_{1,40} = 25.58$, $p \leq 0.001$) but not the rainy season ($R^2 = 0.01$, $F_{1,14} = 0.05$, $p = 0.825$) (Figure 3B). There were no significant relationships between fish length (mm) and muscle or eye δ^{34}S, and liver δ^{13}C or δ^{15}N (Figure 3).

Differences in fish resource use between size groups and seasons were then determined using mixed-effects models within a Bayesian framework, which also provides a marginal and a conditional R^2 value (Table 1). Marginal R^2 ($R^2{}_M$) describes the proportion of model variance that is explained by the fixed effects (i.e., size, season, and their interaction), while conditional R^2 ($R^2{}_C$) describes the proportion of model variance that is explained by both the fixed and the random (i.e., including site) effects. For muscle tissue δ^{13}C, there was a significant effect on size, and there was a significant interaction between size and season (mean ± SD, small dry: −17.57 ± 0.82 and rainy: −16.25 ± 0.20; large dry: −16.41 ± 0.48 and rainy: −16.24 ± 0.55), while for muscle δ^{15}N, there was only a significant effect of size (mean ± SD, small: 9.64 ± 0.29; l: 10.07 ± 0.29). Marginal R^2 values confirmed that the fixed effects size and season described a good proportion of the variability in δ^{13}C ($R^2{}_M = 0.46$), but less so for δ^{15}N ($R^2{}_M = 0.26$; Table 1).

The patterns were similar in eye tissue. For eye δ^{13}C, there was a significant effect of size, season, and a significant interaction between size and season (mean ± SD, small dry: −18.47 ± 0.76 and rainy: −16.87 ± 0.61; large dry: −17.16 ± 0.66 and rainy: −16.13 ± 0.46). For δ^{15}N, there was only a significant effect of size (mean ± SD, small: 7.95 ± 0.40; large: 9.06 ± 0.36). Season and size described a high proportion of the variance in eye δ^{13}C ($R^2{}_M = 0.55$) and also δ^{15}N ($R^2{}_M = 0.51$). There were no significant effects on muscle or eye δ^{34}S, and marginal R^2 values were low ($R^2{}_M$ muscle = 0.02; eye = 0.00). The random effect of site did not describe the variance in muscle δ^{13}C ($R^2{}_C = 0.10$), δ^{15}N ($R^2{}_C = 0.12$), or δ^{34}S ($R^2{}_C = 0.06$), or in eye δ^{13}C ($R^2{}_C = 0.21$) or δ^{15}N ($R^2{}_C = 0.14$), however, it did for eye δ^{34}S ($R^2{}_C = 0.58$) (Table 1).

For liver tissue, patterns were different; there were no significant size or seasonal effects on δ^{13}C or δ^{15}N, and marginal R^2 was low ($R^2{}_M$ δ^{13}C = 0.06; δ^{15}N = 0.11). However, for δ^{34}S, there were significant effects of size and a significant interaction between size and season (mean ± SD, small dry: 23.33 ± 1.28 and rainy: 21.27 ± 0.86; large dry: 22.21 ± 0.62 and rainy: 21.72 ± 1.39). These fixed effects described a higher proportion of the δ^{34}S variance ($R^2{}_M = 0.25$), while the random effect of site described a high proportion of variance across all three isotopes ($R^2{}_C$ δ^{13}C = 0.59; δ^{15}N = 0.24; and δ^{34}S = 0.36) (Table 1). Model results for lipid-corrected liver δ^{34}S values followed the same patterns (Supplementary Figure 1; Supplementary Table 6).

Models run on the raw (uncorrected) δ^{13}C values revealed mostly similar patterns for muscle and eye (Supplementary Table 7). For muscle, there was still a significant effect of size, and for eye, size and season were still significant. However, for both muscle and eye, the interaction between size and season was only marginally significant. For liver raw δ^{13}C, unlike for the corrected values, there were significant effects of size and a significant interaction between size and season (Supplementary Table 6).

Patterns in resource use between seasons were visualized for each size group using a PCA generated from tri-isotope data (δ^{13}C, δ^{15}N, and δ^{34}S). For small fish, seasons were separated largely along with PC1, which explained 58.1% of the variation in the data. This axis was strongly influenced by δ^{13}C. Tissue differences were separated along with PC2 and influenced by δ^{15}N and δ^{34}S. Both dry season liver and eye ellipses, and rainy season liver and eye ellipses overlapped, but there was no seasonal overlap of the same tissue type (Figure 4A). Differences between season ($F_{1,119} = 19.61$, $p < 0.001$), among tissues ($F_{2,119} = 45.75$, $p < 0.001$), and their interaction ($F_{2,119} = 4.51$, $p = 0.003$) were all significant (PERMANOVA, 9,999 permutations).

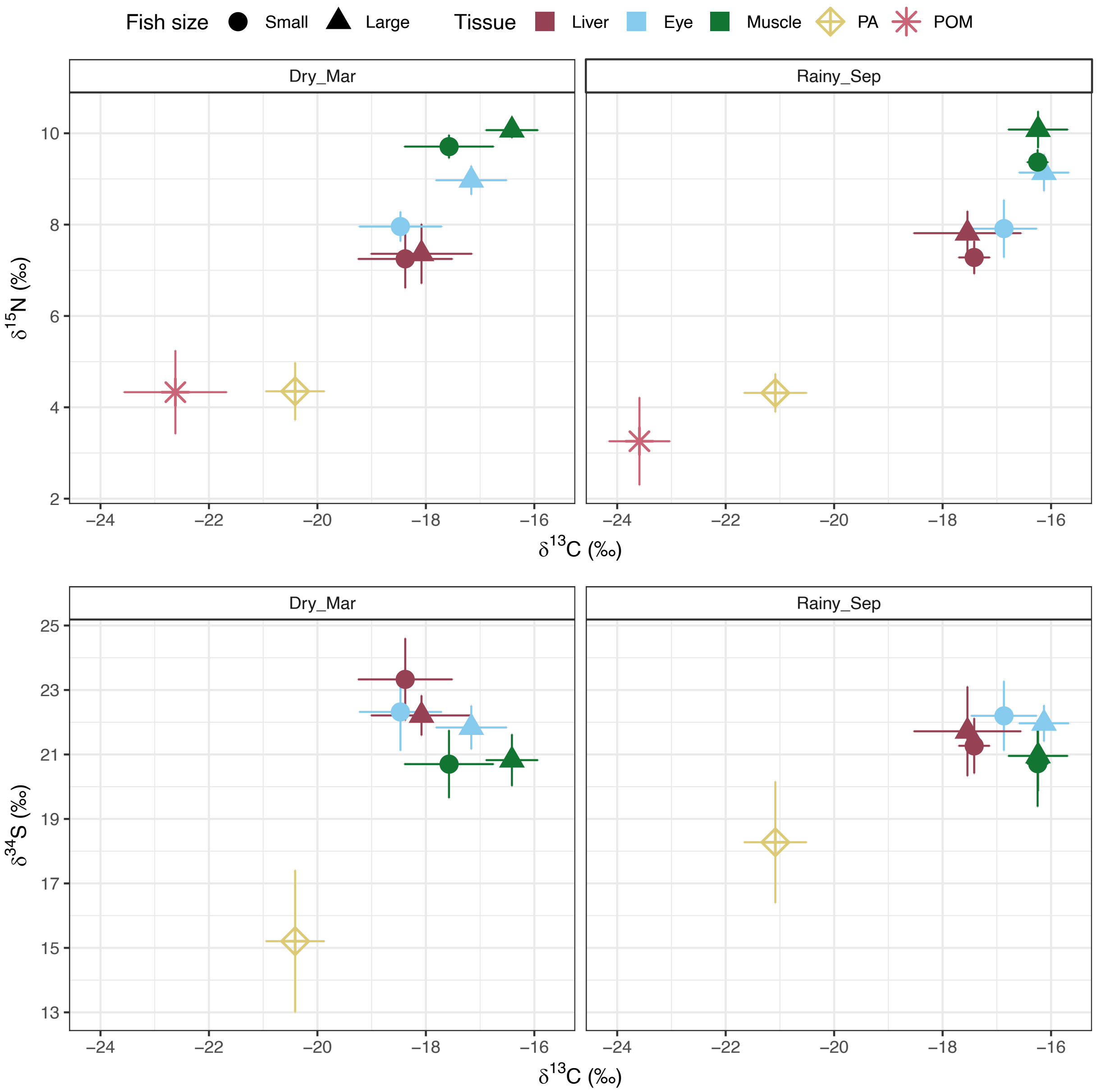

FIGURE 2
Isotope biplots of mean ± standard deviation δ^{13}C and δ^{15}N (top) and δ^{13}C and δ^{34}S (bottom panels) for all samples collected across the five sites in the dry season (March 2013) and the rainy season (September 2012 and 2014). δ^{13}C values are mathematically corrected for high lipid content (see section "Materials and methods"). PA = tunicate, *Polycarpa aurata*. POM, particulate organic matter. Damselfish are either small (<70 mm) or large (>70 mm). Note, no δ^{34}S data are reported for POM (see section "Materials and methods": Sample processing and stable isotope analyses).

For large fish, tissues were separated along PC2 (21.4% of the variation), predominantly influenced by δ^{34}S and δ^{15}N, and differences were significant (PERMANOVA, 9,999 permutations, $F_{1,51}$ = 12.44, $p < 0.001$). δ^{13}C was the primary variable leading to separation along PC1 (Figure 4B). In contrast to the small fish, large-fish ellipses from each season overlapped, with the exception of eye tissue, and, while there was a marginally significant overall difference between seasons (PERMANOVA, 9,999 permutations, $F_{1,51}$ = 3.43, p = 0.03), the interaction between seasons and tissues was not significant ($F_{2,51}$ = 1.07, p = 0.37).

The PCA using the lipid-corrected liver δ^{34}S values revealed a similar separation to the PCA using the raw δ^{34}S values (Supplementary Figure 4). However, unlike the raw values, the PERMANOVA using the corrected δ^{34}S values identified no significant differences among tissues for the large fish; for small

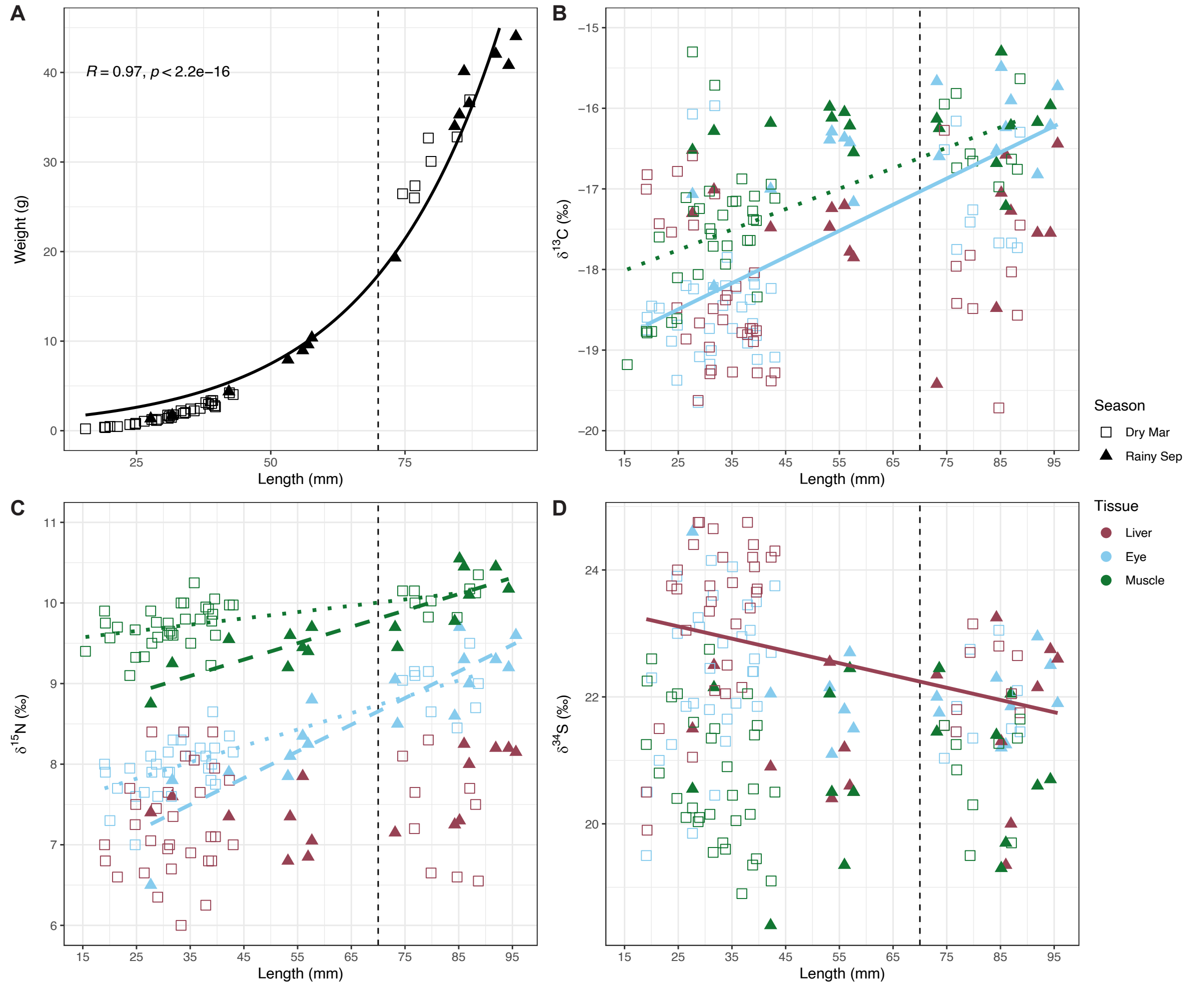

FIGURE 3
Relationships of fish **(A)** weight (g), **(B)** δ^{13}C, **(C)** δ^{15}N, and **(D)** δ^{34}S data plotted against length (mm). For the isotope ratios **(B–D)**, only significant relationships from the regression analysis models are plotted for each tissue. Solid lines represent fish across both seasons (δ^{15}N), dotted lines represent fish in the dry season, and dashed lines represent fish in the rainy season (δ^{13}C and δ^{34}S). δ^{13}C values are mathematically corrected for high lipid content (see section "Materials and methods").

fish, the interaction between season and tissue was no longer significant (Supplementary material).

Suspension feeders and resource availability

There was evidence of seasonality in tunicate δ^{13}C and δ^{34}S as season, and the interaction between season and site had a significant influence on both δ^{13}C (season: $F_{1,47} = 19.54$, $p < 0.001$; season × site: $F_{4,47} = 3.12$, $p = 0.03$) and δ^{34}S (season: $F_{1,47} = 49.82$, $p < 0.001$; season × site: $F_{4,47} = 9.56$, $p < 0.001$) isotope ratios (Supplementary Table 8; Figures 5A,C). While δ^{13}C was higher in the dry season (mean ± SD, −20.41 ± 0.54‰) than in the rainy (−21.08 ± 0.58‰), δ^{34}S was higher in the rainy season (18.28 ± 1.89‰) than the dry (15.21 ± 2.21‰). There were no spatial gradients in either δ^{13}C or δ^{34}S (Supplementary Table 8), but there were significant spatial differences in tunicate δ^{15}N ($F_{4,24} = 3.47$, $p = 0.02$); δ^{15}N was significantly higher at MU compared to MA and SA ($p = 0.02$, respectively). However, δ^{15}N did not vary seasonally (Supplementary Table 8); values were consistent across both dry (4.35 ± 0.63‰) and rainy (4.32 ± 0.42‰) seasons (Figure 5B).

Particulate organic matter δ^{13}C and δ^{15}N varied significantly between seasons ($F_{1,24} = 10.37$, $p = 0.02$ and $F_{1,24} = 9.98$, $p = 0.02$, respectively; Supplementary Table 8; Figures 5D,E), with higher mean δ^{13}C and δ^{15}N in the dry season (δ^{13}C: −22.62 ± 0.95‰; δ^{15}N: 4.33 ± 0.92‰) compared to the rainy season (δ^{13}C: −23.59 ± 0.56‰; δ^{15}N: 3.26 ± 0.96‰). There was

TABLE 1 Mixed-effects model parameter estimates exploring size and seasonal effects on fish δ^{13}C, δ^{15}N, and δ^{34}S.

Predictors	**δ^{13}C**		**δ^{15}N**		**δ^{34}S**	
Muscle (*n* = 3750)	**Estimate**	**95% CI**	**Estimate**	**95% CI**	**Estimate**	**95% CI**
Intercept	−16.44	**−17.00 to −15.89**	10.04	**9.77 to 10.33**	20.86	**20.00 to 21.74**
Small (<70 mm)	−1.12	**−1.65 to−0.58**	−0.34	**−0.58 to −0.07**	−0.16	−0.95 to 0.66
Rainy	0.18	−0.50 to 0.88	0.01	−0.32 to 0.30	0.16	−0.93 to 1.18
Small:Rainy	1.21	**0.34 to 2.11**	−0.32	−0.73 to 0.08	−0.24	−1.54 to 1.10
Random Effects						
Intercept Variance	0.17	0.00 to 0.47	0.05	0.00 to 0.16	0.27	0.00 to 1.01
Residual Variance	0.50	0.33 to 0.69	0.11	0.07 to 0.15	1.19	0.76 to 1.63
Marginal r^2	0.46	0.24 to 0.59	0.26	0.08 to 0.49	0.02	0.00 to 0.14
Conditional r^2	0.56	0.28 to 0.70	0.38	0.19 to 0.71	0.06	0.00 to 0.49
Eye (*n* = 3334)	**Estimate**	**95% CI**	**Estimate**	**95% CI**	**Estimate**	**95% CI**
Intercept	−17.14	**17.95 to −16.36**	8.95	**8.54 to 9.34**	21.83	**20.52 to 23.12**
Small (<70 mm)	−1.24	**−1.67 to −0.78**	−0.97	**−1.31 to −0.65**	0.40	−0.23 to 0.99
Rainy	0.86	**0.31 to 1.44**	0.08	−0.29 to 0.52	0.39	−0.36 to 1.17
Small:Rainy	0.70	**0.01 to 1.49**	−0.09	−0.62 to 0.43	−0.29	−1.25 to 0.71
Random Effects						
Intercept Variance	0.70	0.00 to 2.31	0.12	0.00 to 0.42	2.37	0.00 to 7.38
Residual Variance	0.36	0.22 to 0.50	0.18	0.12 to 0.25	0.66	0.41 to 0.92
Marginal r^2	0.55	0.20 to 0.71	0.51	0.21 to 0.68	0.00	0.00 to 0.10
Conditional r^2	0.76	0.62 to 0.93	0.65	0.45 to 0.82	0.58	0.31 to 0.97
Liver (*n* = 3334)	**Estimate**	**95% CI**	**Estimate**	**95% CI**	**Estimate**	**95% CI**
Intercept	−16.96	**−18.17 to −15.81**	8.40	**7.80 to 9.06**	22.31	**20.87 to 23.73**
Small (<70 mm)	−0.21	−0.64 to 0.32	−0.23	−0.66 to 0.22	0.9	**0.17 to 1.60**
Rainy	0.35	−0.24 to 0.97	0.34	−0.24 to 0.89	−0.29	−1.24 to 0.59
Small:Rainy	0.45	−0.39 to 1.23	−0.62	−1.39 to 0.09	−1.84	**−3.09 to −0.64**
Random Effects						
Intercept Variance	1.73	0.06 to 5.52	0.31	0.00 to 1.00	2.66	0.06 to 7.78
Residual Variance	0.36	0.23 to 0.51	0.34	0.21 to 0.48	0.88	0.53 to 1.22
Marginal r^2	0.06	0.00 to 0.22	0.11	0.01 to 0.27	0.27	0.02 to 0.42
Conditional r^2	0.65	0.45 to 0.99	0.35	0.07 to 0.80	0.63	0.44 to 0.945

δ^{13}C values have been mathematically corrected for high lipid content, and liver δ^{13}C and δ^{15}N have been corrected for tissue-dependent fractionation (see Section "Materials and methods"). Intercept values represent the average isotope value for a large (>70 mm) in the dry season. Estimates are means with 95% credible intervals (CI). Bold indicates non-overlapping CI. Marginal R^2 is the variance explained only by fixed effects, conditional R^2 is the variance explained by the entire model (fixed and random effects).

no significant effect of site, or of the interaction between season and site, on either δ^{13}C or δ^{15}N (**Supplementary Table 8**).

In contrast, while there was no seasonality in concentrations of POC and PON, there was a significant spatial gradient. For POC and PON, season, the interaction between seasons, and site, were non-significant (ANOVA, $p > 0.05$), while the effect of site was significant (POC: $F_{10,24} = 5.78$, $p = 0.02$; PON: $F_{10,24} = 8.08$, $p = 0.006$). Tukey's *post hoc* analyses revealed that this was driven exclusively by MU which had significantly higher POC (mean POC µg/L: MU 22.91, MB 9.11, BA 6.94, MA 6.23, SA 8.48) and PON (mean PON µg/L: MU 3.33, MB 1.22, BA 1.01, MA 0.81, SA 1.14) concentrations compared to the other sites.

Discussion

In the dynamic environment of coral reef ecosystems, resource availability may fluctuate markedly both spatially and temporally, with implications for associated food webs. Here, across a semi-enclosed tropical embayment in the Philippines, we did not see the expected spatial gradient in fish tissue isotopes (e.g., Wyatt et al., 2012b; Gajdzik et al., 2016; McMahon et al., 2016; Miller et al., 2019), despite the apparent hydrographic separation of sites with varying degrees of oceanic exposure. Instead, there appeared to be pronounced seasonal fluctuations in food web dynamics associated with the rainy and dry seasons, which was evident in the underlying resources (i.e., POM).

These fluctuations were reflected in resource use by suspension feeding primary consumers (i.e., tunicates) but only in some secondary consumers (i.e., small but not large damselfish), a pattern that only became pronounced through analysis of $\delta^{34}S$ as a third isotopic tracer.

Size and seasonal effects on isotope ratios in fish tissues

Small and large damselfish appeared to differ in their resource use, indicating that they might employ different feeding strategies with ontogeny. For example, there was a significant seasonal difference in the isotope ratios of small fish tissues, particularly muscle and eye $\delta^{13}C$, which were more enriched in the rainy season, and liver $\delta^{34}S$, which was lower in the rainy season. Taken together, these data are indicative of smaller fish benefitting from more benthic food chains during the rainy season. During the dry season, when phytoplankton production and chlorophyll *a* in the embayment are higher (San Diego-McGlone et al., 1995), there was evidence of greater reliance on oceanic food chains. In contrast, for the larger fish, isotope ratios of all tissues were similar between seasons, suggesting movement toward a seasonally consistent feeding strategy with age. The more enriched $\delta^{13}C$ and lower $\delta^{34}S$ of large fish tissues further indicated that they may preferentially target benthic invertebrates, possibly reflecting increased foraging movements away from coral heads (Nash et al., 2015). While size-based differences in *Dascyllus* feeding strategies have previously been recorded, they were not always comparable to those found here. In Madagascar, smaller individuals of *Dascyllus aruanus* fed on benthic prey, while larger individuals fed on more planktonic prey (Frédérich et al., 2010), perhaps reflecting the smaller adult size of *D. aruanus* (Kulbicki et al., 2005) and high site fidelity throughout their life span. *D. trimaculatus* larger adult body size might support increased local foraging area, explaining observations that they have some of the highest $\delta^{15}N$ values and the most variable $\delta^{13}C$ values across a range of sizes (Frédérich et al., 2009). Clearly, size-based differences in damselfish resource use and feeding strategies may not always be consistent between species and systems (Eurich et al., 2019) and may be impossible to detect without additional tracers such as $\delta^{34}S$ (see below). However, regardless of size, fish C:N ratios were consistently higher in the dry season across all tissues (**Supplementary Figure 3**), and this was particularly pronounced in liver tissue. Higher lipid levels are linked to better overall condition, suggesting that the food chains that the fish were accessing in the dry season were most beneficial to their growth. As the presence of lipids can influence stable isotope values, mathematical corrections were applied to the data to account for this. While the models run on the raw $\delta^{13}C$ values revealed similar patterns in muscle and eye tissue, for liver the outputs were very different: size and season had no effect on corrected liver $\delta^{13}C$, but for the raw values, size and size interacting with season were highly significant. This confirms that higher tissue lipid content can influence $\delta^{13}C$ values, so correcting the values is a more conservative approach that reduces the confounding influence that lipids may have on interpreting patterns.

Correcting for tissue-dependent fractionation allowed direct comparison of seasonal effects across the three tissue types without the confounding factor of varying isotopic discrimination. There was pronounced seasonality in all three tissues for small fish. While evidence of dietary shifts across seasons was expected in the faster turnover liver, there was also clear seasonal variation detected in both muscle and eye tissue. Muscle is a longer turnover tissue, reflecting a dietary time frame of several weeks to months in the body size range relevant here [mean turnover $\delta^{13}C$ at 28°C temperature (Iizuka et al., 2009)]: Small 39.5 days, Large 67.9 days; (Thomas and Crowther, 2015) but the dietary time frame of whole fish eye tissue is not well constrained. Here, the size and seasonal patterns of fish muscle and eye tissue $\delta^{13}C$ were comparable, and eye $\delta^{15}N$ was consistently lower than muscle $\delta^{15}N$. This correlates with one of the few studies to consider fish eye tissue (including retina), which found a significant positive correlation between fish muscle and eye $\delta^{13}C$ (with a regression relationship close to 1:1), and that eye $\delta^{15}N$ was consistently lower ($\sim$2‰) than muscle $\delta^{15}N$ (Kanaya et al., 2019). This suggests that whole eye tissue may represent a similar dietary time frame to that of muscle (i.e., weeks to months). However, evidence of seasonal variation in consumer resource use is less expected in longer turnover tissues. One explanation for the observed variation, is that fish samples were collected mid-season; rainy season samples were collected in September, but higher rainfall associated with the summer monsoon begins in June (Wang and LinHo, 2002). As such, given the calculated turnover rates for the sampled tissues (see above), the damselfish had already begun to assimilate resources available to them during the initial few months of the rainy season. Similarly, dry season samples were collected in March, but the dry season extends from November to May; fish likely already integrated dry season resources that were then reflected in their longer turnover tissues. Moreover, the calculated turnover rates for both size groups indicate that their tissues reflect the same season, further confirming the discrepancies between their foraging strategies. Careful consideration of tissue turnover times in the context of environmental dynamics is required, especially in the absence of analysis of "fast" turnover tissues with higher temporal resolution.

Surprisingly, while there were significant differences in small fish muscle and eye $\delta^{13}C$ between seasons, seasonal $\delta^{13}C$ differences in "fast" liver tissues were not significant. Similar to muscle and eye, liver $\delta^{13}C$ was more depleted in the dry compared to the rainy season, but there was a notable exception of the samples from the innermost site in the port of Muelle

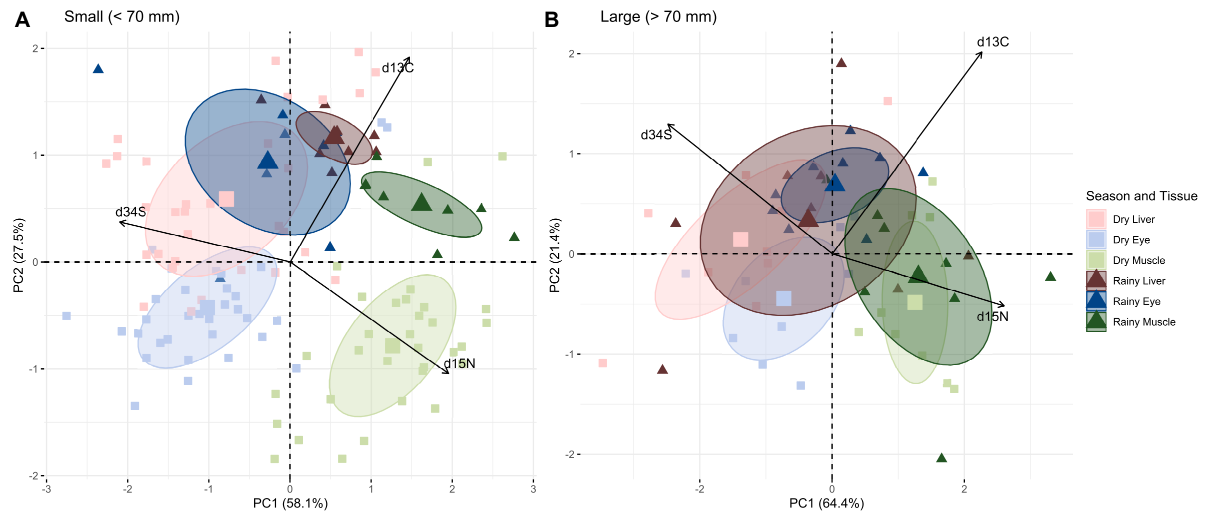

FIGURE 4

Principal component analysis (PCA) of **(A)** small (<70 mm) and **(B)** large (>70 mm) damselfish δ^{13}C, δ^{15}N, and δ^{34}S values from the liver, eye, and muscle tissues collected from five sites across the embayment in the dry season (March) and the rainy season (September). δ^{13}C values are mathematically corrected for high lipid content, and liver δ^{13}C and δ^{15}N are corrected for tissue-dependent fractionation (see section "Materials and methods"). Ellipses are 95% confidence ellipses with centroids. Variables are overlaid as vectors with arrows.

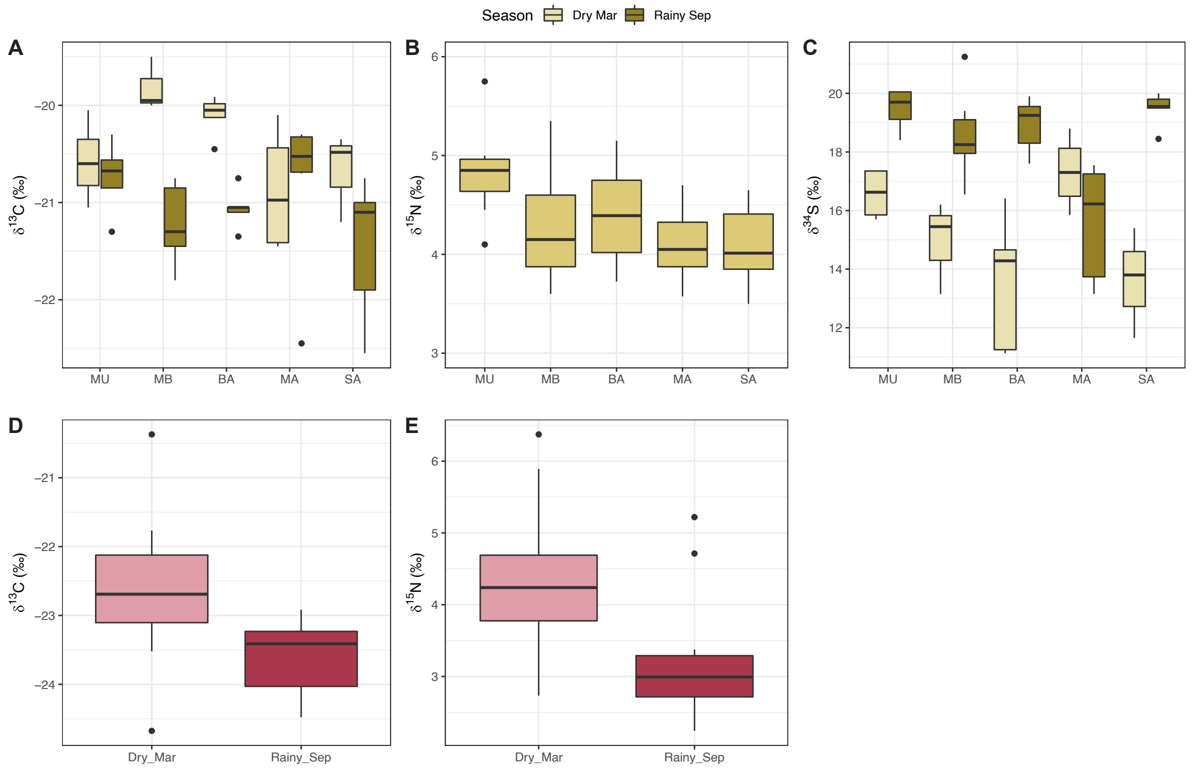

FIGURE 5

Stable isotope ratios of panels **(A–C)** tunicates (*Polycarpa aurata*) and panels **(D,E)** particulate organic matter (POM) sampled across Puerto Galera embayment. Data are pooled based on whether there were significant differences among groups or not. Tunicate δ^{15}N varied spatially, δ^{13}C and δ^{34}S seasonally and with an interaction between season and site; POM δ^{13}C and δ^{15}N varied only seasonally. Note, no δ^{34}S data are reported for POM.

(MU). At MU, dry season liver δ^{13}C values were comparable to those in the rainy season (more enriched). MU, being the most sheltered inshore site, has reduced water flow and is heavily influenced by surrounding terrestrial and anthropogenic inputs (Iizuka et al., 2009), evidenced by the higher concentrations of POC and PON. More consistent benthic foraging, i.e., enriched δ^{13}C values, at this site may have precluded a significant seasonal difference in liver δ^{13}C values from being observed. In contrast to δ^{13}C, small fish liver δ^{34}S values were significantly lower in the rainy season (~21.3‰) than in the dry season (~23.5‰), indicative of a seasonal difference in the food web baseline. There was no corresponding seasonal shift in muscle or eye δ^{34}S, which likely relates to the longer dietary time frames that these tissues represent. The lower δ^{34}S values in the fast turnover liver in the rainy season are suggestive of fluxes of terrestrial material entering the food web, likely from increased run-off (San Diego-McGlone et al., 1995). However, δ^{34}S takes longer than δ^{13}C or δ^{15}N to reach equilibrium in muscle tissue (Barnes and Jennings, 2007), and assuming that the turnover of eye tissue is similar, this may explain the absence of seasonal δ^{34}S variation in these two tissues. It is important to note also that high lipid content in liver tissues might have influenced the δ^{34}S values. While the patterns using the lipid-corrected δ^{34}S values were similar to those using the raw δ^{34}S values, seasonal effects were less pronounced. Unfortunately, the only current known δ^{34}S lipid correction factor derives from shark liver (Riverón et al., 2022), so it is not clear how appropriate this value is for planktivorous damselfish. Regardless, a better understanding of how lipid levels in tissues might influence δ^{34}S values is sorely needed. Finally, it is important to also consider sample sizes when interpreting this pattern. Here, opportunistic sampling led to an unbalanced sampling design; there were fewer small fish encountered during the rainy season than the dry season, and, notably, none were observed at MU or Sabang (SA). Though the patterns observed in this study strongly suggest that small fish vary in their resource use between seasons, future work would benefit from incorporating additional samples across the embayment to further explore these spatial and seasonal food web dynamics using the multi-tissue, multi-isotope approach.

Patterns in δ^{15}N values were as expected but not highly informative regarding changes in resource use. Many food web studies have a strong focus on δ^{15}N analysis (Skinner et al., in press), but this tracer may not always be the most informative for understanding resource use in coral reef food webs (Miyajima and Umezawa, 2010). Here, there were significant differences between small and large fish δ^{15}N, and values increased with body size. Body size and δ^{15}N relationships are well studied in marine food webs but not always evident (Layman et al., 2005; Al-Habsi et al., 2008; Jennings et al., 2008; Zhu et al., 2019). Increasing δ^{15}N with body size suggested larger individuals exploited higher trophic position prey, possibly due to changes in their habitat use or fitness, or increased gape size (Munday, 2001; Newman et al., 2012). For fish from both size groups, there was evidence of tissue-specific discrimination that correlated well with previous studies; fish muscle was enriched in δ^{15}N compared to the liver (Pinnegar and Polunin, 1999; Chen et al., 2012) and eye (Kanaya et al., 2019), but applying corrections to account for tissue-dependent fractionation allowed direct comparisons of seasonal effects across tissues. There was no seasonality in the δ^{15}N values of any of the tissues of either size group, suggesting that they are consistently feeding on prey of a similar trophic position across seasons with no change in the underlying δ^{15}N baseline values. Although useful for determining consumer trophic position, δ^{15}N may not be as informative for detecting seasonal changes in consumer resource use.

Suspension feeders as indicators of resource availability

Tunicates were sampled across the embayment to better characterize the planktonic production pathway and how this might vary seasonally. While some patterns in the tunicate tissues clearly reflected those of the damselfish, others were less easy to reconcile. For example, similar to the small damselfish, there were no seasonal patterns in tunicate δ^{15}N, but highly seasonal patterns in tunicate δ^{13}C and δ^{34}S. However, the patterns in δ^{13}C and δ^{34}S were reversed; tunicate δ^{13}C was more enriched and δ^{34}S was lower in the dry season, indicative of reliance on nearshore production pathways. This is because there is a distinct spatial gradient in δ^{34}S values related to the biogeochemical cycling of sulfur; offshore marine sulfate values are close to 21‰, while in anaerobic and anoxic sediments in coastal environments, sulfate is reduced to hydrogen sulfide which has lower δ^{34}S values (Fry et al., 1982; Fry, 1986; Peterson, 1999). As such, lower tunicate δ^{34}S in the dry season (coupled with more enriched δ^{13}C) indicate reliance on suspended material derived from benthic organic matter or sulfur-oxidizing bacteria (Peterson et al., 1986; Oakes and Connolly, 2004). In contrast, small damselfish tissues in the dry season indicated a response to the increased phytoplankton production and chlorophyll *a* concentrations that tend to prevail in this season (San Diego-McGlone et al., 1995). Tunicates, as suspension feeders, are often sampled to represent a time-integrated pelagic baseline, which is less variable than POM (Stowasser et al., 2012; Ménard et al., 2014); however, the dietary time frame that their tissues represent is not well known. Furthermore, recent evidence suggests that they may instead consume microbes, thus making it inappropriate to use them as representatives of the pelagic food chain (Pakhomov et al., 2019). Indeed, other suspension feeders, such as oysters, are known to preferentially select food particles (Newell and Jordan, 1983), suggesting that the tunicates may not be consuming all of the suspended POM. In addition, the damselfish occupy a higher trophic position than the tunicates, suggesting that seasonal variations observed in the tunicates may have been different from those obscured in the damselfish, as these were diminished across trophic linkages. These caveats may explain the discrepancy between the damselfish and tunicate $\delta^{13}C$ and $\delta^{34}S$ patterns, further confirming that caution is needed when using tunicates as a "pelagic" baseline in reef food web studies. However, regardless of the food chain they represent, there was strong evidence of seasonality in their tissues consistent with the small damselfish, likely linked to fluctuations in resource availability between the rainy and dry seasons.

Particulate organic matter samples confirmed that suspended resources varied seasonally across the embayment. POM $\delta^{15}N$ was higher in the dry season, likely linked to pools of accumulated ammonia from anthropogenic waste (San Diego-McGlone et al., 1995). Similar to the tunicates, POM $\delta^{13}C$ was more enriched in the dry season, consistent with reduced terrestrial inputs (which have very depleted $\delta^{13}C$: −31 to −25‰; Mackensen and Schmiedl, 2019) due to lower rainfall. Differences in $\delta^{13}C$ values between seasons could relate to water temperature though, as isotopic fractionation of planktonic $\delta^{13}C$ decreases in warmer water, leading to more enriched values. Here, however, POM $\delta^{13}C$ values were more enriched in the dry season when water temperatures were lower. Furthermore, water temperatures varied by only 2°C between seasons, corresponding to a difference in fractionation of only 0.70‰ (0.35‰ per °C; Fontugne and Duplessy, 1981). This suggests that observed seasonal differences in $\delta^{13}C$ were not driven by differences in water temperature. Indeed, changes in phytoplankton $\delta^{13}C$ fractionation may also arise from differences in light conditions (intensity and duration) and nutrients (Brandenburg et al., 2022). These factors may be more relevant here than the temperature for explaining differences in $\delta^{13}C$ of POM (phytoplankton) between the rainy and dry seasons. It seems that the POM data reflect some aspects of the benthic food chain; the snapshot nature of POM sampling coupled with the dynamic environment of the embayment, i.e., variable flushing rates influencing residence times and accumulated nutrients (San Diego-McGlone et al., 1995; Iizuka et al., 2009), may influence oceanic contributions evident from POM $\delta^{13}C$. The lack of seasonal variation in POC and PON concentrations could suggest that the change in resources may be of a similar magnitude, leading to variations in POM isotope ratios but not in concentrations (Wyatt et al., 2013). Interestingly, despite distinct temporal differences, there was no significant spatial isotopic gradient in POM $\delta^{13}C$ or $\delta^{15}N$ and the spatial variation in POC and PON was driven solely by the most inshore site (MU). Although the mechanisms through which these food chains fluctuate and become available to primary and secondary consumers across the embayment remains unclear, it appears that this is predominantly a seasonally fluctuating system rather than a spatial one as previously assumed.

Incorporating $\delta^{34}S$ as a third isotope for exploring food web dynamics

Sulfur isotope ratios ($\delta^{34}S$) are increasingly being recommended as a useful third tracer for stable isotope food web studies (Connolly et al., 2004; Skinner et al., 2019a). Our data further support this; $\delta^{34}S$ was instrumental in identifying short-term resource use changes of small fish (as reflected in their liver tissues) but was also important for highlighting strong seasonal variation in the suspension-feeding tunicates. The lack of seasonal $\delta^{34}S$ variation in large fish argues against a simple seasonal change in the $\delta^{34}S$ baselines of this system, instead suggesting small fish and tunicates are utilizing different resources in each season. While larger fish may have a slower isotopic turnover, particularly in their muscle tissue, we would still expect to see changes in their liver $\delta^{34}S$ due to its faster turnover. Unfortunately, no POM $\delta^{34}S$ data are available to explore seasonal shifts in the underlying suspended resources that may be evident with sulfur. In this system, it seems that while $\delta^{13}C$ and $\delta^{34}S$ are key to understanding seasonal fluxes (Connolly et al., 2004; Briand et al., 2015), $\delta^{15}N$ may be less valuable, highlighting the utility of adding tracers like $\delta^{34}S$, especially in systems with minimal nitrogen isotope variation.

Conclusion

Investigations into seasonality in aquatic food webs are increasing (Wantzen et al., 2002; Cobain et al., 2022), but there is still limited understanding of how varying fluxes translate into variation in reef food webs (but see Briand et al., 2015), with the majority of coral reef stable isotope studies conducted during limited temporal windows and focusing on one or two tracers in a single tissue (Skinner et al., in press). Our data suggest that coral reef food web resources and consumer trophodynamics can vary substantially between seasons even over small spatial scales. Restricting sampling to a single period may therefore overlook important seasonal food web dynamics, which could alter our interpretation of production source pathways and consumer resource use. Furthermore, combining multiple isotopic tracers ($\delta^{13}C$, $\delta^{15}N$, and $\delta^{34}S$) with the analysis of separate tissue types (representing different dietary time frames, e.g., Wyatt et al., 2019) proved instrumental in identifying temporal changes in consumer dietary variation. Where lethal sampling is already occurring, we strongly recommend that researchers maximize the dietary information obtained from each individual by sampling a range of tissue types with different turnover times. In addition, given the ease at which $\delta^{34}S$ can now be measured along with $\delta^{13}C$ and $\delta^{15}N$, and the important food chain information it can convey (Connolly et al., 2004), we suggest that marine food web studies employ a tri-isotope approach by default. However, more research into the effect of tissue lipid levels on $\delta^{34}S$ is sorely needed. As coral reefs are currently experiencing unprecedented worldwide declines (Hoegh-Guldberg et al., 2017; Hughes et al., 2017; Darling et al., 2019), improved quantification of food web dynamics across both fine and broad spatial and temporal scales is urgently needed.

Data availability statement

The raw data supporting the conclusions of this article will be made available by the authors, without undue reservation.

Ethics statement

This study was approved by Prior Informed Consent from the Municipality of Puerto Galera (PIC Certificate, Document No. 146, September 25, 2012) and a Gratuitous Permit from the Philippines Department of Agriculture (GP-No. 0073-14).

Author contributions

AW conceptualized the study and collected the samples with assistance from NM and TM. AW and CS formulated the statistical analyses and developed the methodology. Y-DP and CS processed the samples. CS analyzed the data and wrote the first draft of the manuscript. All authors contributed substantially to revisions.

Funding

Field collections were supported by the Coastal Ecosystem Conservation and Adaptive Management under Local and Global Environmental Impacts in the Philippines (CECAM) project supported by the "Science and Technology Research Partnership for Sustainable Development (SATREPS)" scheme jointly funded by the Japan Science and Technology Agency and the Japan International Cooperation Agency (JICA) to K. Nadaoka and M. D. Fortes. AW was supported during field work by a fellowship from the Japan Society for the Promotion of Science. Sample analysis was supported by funding from the Hong Kong Branch of the Southern Marine Science and Engineering Guangdong Laboratory (Guangzhou) (SMSEGL20SC01) to AW. Y-DP was supported by the Asian Future Leaders Scholarship Program, jointly contributed by The Hong Kong University of Science and Technology and Bai Xian Asia Institute.

Acknowledgments

We sincerely thank the Municipality of Puerto Galera, the JICA Philippines Office, including Y. Nagahama and Y. Geroleo, and the CECAM project coordinating office for logistical support in the field. R. M. Magturo of Sandbar Divers provided diving support. We also thank M. R. D. Cobain for helpful discussion regarding the analysis and the two reviewers for their helpful feedback which improved the manuscript.

Conflict of interest

The authors declare that the research was conducted in the absence of any commercial or financial relationships that could be construed as a potential conflict of interest.

Publisher's note

Supplementary material

The Supplementary Material for this article can be found online at: https://www.frontiersin.org/articles/10.3389/fevo.2022.942968/full#supplementary-material

References

Al-Habsi, S., Sweeting, C., Polunin, N., and Graham, N. (2008). δ15N and δ13C elucidation of size-structured food webs in a Western Arabian Sea demersal trawl assemblage. *Marine Ecol. Prog. Series* 353, 55–63. doi: 10.3354/meps07167

Allen, G. R. (1991). *Damselfishes of the World*. Melle: Mergus.

Barnes, C., and Jennings, S. (2007). Effect of temperature, ration, body size and age on sulphur isotope fractionation in fish. *Rapid Commun. Mass Spectrom.* 21, 1461–1467. doi: 10.1002/rcm.2982

Bates, D., Maechler, M., Bolker, B., and Walker, S. (2015). Fitting Linear Mixed-Effects Models Using lme4. *J. Statist. Softw.* 67, 1–48.

Bell-Tilcock, M., Jeffres, C. A., Rypel, A. L., Sommer, T. R., Katz, J. V. E., Whitman, G., et al. (2021). Advancing diet reconstruction in fish eye lenses. *Meth. Ecol. Evol.* 12, 449–457. doi: 10.1111/2041-210X.13543

Boecklen, W. J., Yarnes, C. T., Cook, B. A., and James, A. C. (2011). On the Use of Stable Isotopes in Trophic Ecology. *Annu. Rev. Ecol. Evol. System.* 42, 411–440. doi: 10.1146/annurev-ecolsys-102209-144726

Booth, D. J. (1995). Juvenile Groups in a Coral-Reef Damselfish: Density-Dependent Effects on Individual Fitness and Population Demography. *Ecology* 76, 91–106. doi: 10.2307/1940634

Brandenburg, K. M., Rost, B., Van de Waal, D. B., Hoins, M., and Sluijs, A. (2022). Physiological control on carbon isotope fractionation in marine phytoplankton. *Biogeosciences* 19, 3305–3315. doi: 10.5194/bg-19-3305-2022

Briand, M. J., Bonnet, X., Goiran, C., Guillou, G., and Letourneur, Y. (2015). Major Sources of Organic Matter in a Complex Coral Reef Lagoon: Identification from Isotopic Signatures (δ13C and δ15N). *PLoS One* 10:e0131555. doi: 10.1371/journal.pone.0131555

Canseco, J. A., Niklitschek, E. J., and Harrod, C. (2022). Variability in δ13C and δ15N trophic discrimination factors for teleost fishes: A meta-analysis of temperature and dietary effects. *Rev. Fish Biol. Fish.* 32, 313–329. doi: 10.1007/s11160-021-09689-1

Carreón-Palau, L., Parrish, C. C., del Angel-Rodríguez, J. A., Pérez-España, H., and Aguiñiga-García, S. (2013). Revealing organic carbon sources fueling a coral reef food web in the Gulf of Mexico using stable isotopes and fatty acids. *Limnol. Oceanogr.* 58, 593–612. doi: 10.4319/lo.2013.58.2.0593

Chen, G., Zhou, H., Ji, D., and Gu, B. (2012). Stable isotope enrichment in muscle, liver, and whole fish tissues of brown-marbled groupers (Epinephelus fuscoguttatus). *Ecol. Process.* 1:7. doi: 10.1186/2192-1709-1-7

Cobain, M. R., McGill, R. A., and Trueman, C. N. (2022). Stable isotopes demonstrate seasonally stable benthic-pelagic coupling as newly fixed nutrients are rapidly transferred through food chains in an estuarine fish community. *J. Fish. Biol.* [Epub ahead of print]. doi: 10.1111/jfb.15005

Cocheret de la Morinière, E., Pollux, B. J. A., Nagelkerken, I., Hemminga, M. A., Huiskes, A. H. L., and Van der Velde, G. (2003). Ontogenetic dietary changes of coral reef fishes in the mangrove-seagrass-reef continuum: Stable isotopes and gut-content analysis. *Mar. Ecol. Prog. Series* 246, 279–289. doi: 10.3354/meps246279

Connolly, R. M., Guest, M. A., Melville, A. J., and Oakes, J. M. (2004). Sulfur stable isotopes separate producers in marine food-web analysis. *Oecologia* 138, 161–167. doi: 10.1007/s00442-003-1415-0

Cummings, D. O., Booth, D. J., Lee, R. W., Simpson, S. J., and Pile, A. J. (2010). Ontogenetic diet shifts in the reef fish Pseudanthias rubrizonatus from isolated populations on the North-West Shelf of Australia. *Mar. Ecol. Prog. Series* 419, 211–222. doi: 10.3354/meps08827

Darling, E. S., McClanahan, T. R., Maina, J., Gurney, G. G., Graham, N. A. J., and Januchowski-Hartley, F. (2019). Social–environmental drivers inform strategic management of coral reefs in the Anthropocene. *Nat. Ecol. Evol.* 3, 1341–1350. doi: 10.1038/s41559-019-0953-8

Davis, J. P., Pitt, K. A., Fry, B., and Connolly, R. M. (2015). Stable isotopes as tracers of residency for fish on inshore coral reefs. *Estuar. Coast. Shelf Sci.* 167, 368–376. doi: 10.1016/j.ecss.2015.10.013

Erler, D. V., Shepherd, B. O., Linsley, B. K., Nothdurft, L. D., Hua, Q., and Lough, J. M. (2019). Has Nitrogen Supply to Coral Reefs in the South Pacific Ocean Changed Over the Past 50 Thousand Years? *Paleoceanogr. Paleoclimatol.* 34, 567–579. doi: 10.1029/2019PA003587

Eurich, J. G., Matley, J. K., Baker, R., McCormick, M. I., and Jones, G. P. (2019). Stable isotope analysis reveals trophic diversity and partitioning in territorial damselfishes on a low-latitude coral reef. *Mar. Biol.* 166:17. doi: 10.1007/s00227-018-3463-3

Fey, P., Parravicini, V., Bănaru, D., Dierking, J., Galzin, R., Lebreton, B., et al. (2021). Multi-trophic markers illuminate the understanding of the functioning of a remote, low coral cover Marquesan coral reef food web. *Sci. Rep.* 11:20950. doi: 10.1038/s41598-021-00348-w

Fontugne, M. R., and Duplessy, J.-C. (1981). Organic carbon isotopic fractionation by marine plankton in the temperature range -1 to 31°C. *Oceanol. Acta* 4, 85–90.

Frédérich, B., Fabri, G., Lepoint, G., Vandewalle, P., and Parmentier, E. (2009). Trophic niches of thirteen damselfishes (Pomacentridae) at the Grand Récif of Toliara. *Madagascar. Ichthyol. Res.* 56, 10–17. doi: 10.1007/s10228-008-0053-2

Frédérich, B., Lehanse, O., Vandewalle, P., and Lepoint, G. (2010). Trophic Niche Width, Shift, and Specialization of Dascyllus aruanus in Toliara Lagoon, Madagascar. *Copeia* 2, 218–226. doi: 10.1643/CE-09-031

Frédérich, B., Olivier, D., Gajdzik, L., and Parmentier, É. (2016). "Trophic Ecology of Damselfishes," in *Biology of Damselfishes*, eds B. Frédérich and E. Parmentier (Boca Raton, FL: CRC Press). doi: 10.1201/9781315373874

Fry, B. (1986). Stable Sulfur Isotopic Distributions and Sulfate Reduction in Lake Sediments of the Adirondack Mountains, New York. *Biogeochemistry* 2, 329–343. doi: 10.1007/BF02180324

Fry, B., Scalan, R. S., Winters, J. K., and Parker, P. L. (1982). Sulphur uptake by salt grasses, mangroves, and seagrasses in anaerobic sediments. *Geochim. Cosmochim. Acta* 46, 1121–1124. doi: 10.1016/0016-7037(82)90063-1

Gajdzik, L., Parmentier, E., Sturaro, N., and Frédérich, B. (2016). Trophic specializations of damselfishes are tightly associated with reef habitats and social behaviours. *Mar. Biol.* 163:249. doi: 10.1007/s00227-016-3020-x

Greenwood, N. D. W., Sweeting, C. J., and Polunin, N. V. C. (2010). Elucidating the trophodynamics of four coral reef fishes of the Solomon Islands using δ15N and δ13C. *Coral Reefs* 29, 785–792. doi: 10.1007/s00338-010-0626-1

Haas, A. F., Naumann, M. S., Struck, U., Mayr, C., el-Zibdah, M., and Wild, C. (2010). Organic matter release by coral reef associated benthic algae in the Northern Red Sea. *J. Exper. Mar. Biol. Ecol.* 389, 53–60. doi: 10.1016/j.jembe.2010.03.018

Hadfield, J. D. (2010). MCMC Methods for Multi-Response Generalized Linear Mixed Models: The MCMCglmm R Package. *J. Statist. Softw.* 33, 1–22. doi: 10.18637/jss.v033.i02

Hagen, W. (1988). On the significance of lipids in Antarctic zooplankton. *Ber Polarforsch* 49, 1–117.

Hoegh-Guldberg, O., and Dove, S. (2008). "Primary production, nutrient recycling and energy flow through coral reef ecosystems,". In *The Great Barrier Reef: Biology, Environment and Management* M. Kingsford, O. Hoegh-Guldberg, P. Hutchings (Clayton: CSIRO publishing)59–73.

Hoegh-Guldberg, O., Poloczanska, E. S., Skirving, W., and Dove, S. (2017). Coral Reef Ecosystems under Climate Change and Ocean Acidification. *Front. Mar. Sci.* 4:158. doi: 10.3389/fmars.2017.00158

Hughes, T. P., Kerry, J. T., Álvarez-Noriega, M., Álvarez-Romero, J. G., Anderson, K. D., and Baird, A. H. (2017). Global warming and recurrent mass bleaching of corals. *Nature* 543, 373–377. doi: 10.1038/nature21707

Iizuka, H., Tamura, H., Pokavanich, T., Rubio-Paringit, M. C. D., Nadaoka, K., and Fortes, M. D. (2009). Highly Skewed Tidal Circulation Pattern and Water Quality in Puerto Galera Bay. Mindoro Island, Philippines. *Coast. Eng. J.* 51, 341–361. doi: 10.1142/S0578563409002065

Jennings, S., Barnes, C., Sweeting, C. J., and Polunin, N. V. C. (2008). Application of nitrogen stable isotope analysis in size-based marine food web and macroecological research. *Rapid Commun. Mass Spectrom.* 22, 1673–1680. doi: 10.1002/rcm.3497

Kanaya, G., Solovyev, M. M., Shikano, S., Okano, J.-I., Ponomareva, N. M., and Yurlova, N. I. (2019). Application of stable isotopic analyses for fish host–parasite systems: An evaluation tool for parasite-mediated material flow in aquatic ecosystems. *Aqua. Ecol.* 53, 217–232. doi: 10.1007/s10452-019-09684-6

Kiljunen, M., Grey, J., Sinisalo, T., Harrod, C., Immonen, H., and Jones, R. I. (2006). A revised model for lipid-normalizing δ13C values from aquatic organisms, with implications for isotope mixing models. *J. Appl. Ecol.* 43, 1213–1222. doi: 10.1111/j.1365-2664.2006.01224.x

Kulbicki, M., Guillemot, N., and Amand, M. (2005). A general approach to length-weight relationships for New Caledonian lagoon fishes. *Cybium* 29, 235–252.

Layman, C. A., Winemiller, K. O., Arrington, D. A., and Jepsen, D. B. (2005). Body size and trophic position in a diverse tropical food web. *Ecology* 86, 2530–2535. doi: 10.1890/04-1098

Lê, S., Josse, J., and Husson, F. (2008). FactoMineR: An R Package for Multivariate Analysis. *J. Statist. Softw.* 25:18. doi: 10.18637/jss.v025.i01

Letourneur, Y., Briand, M. J., and Graham, N. A. J. (2017). Coral reef degradation alters the isotopic niche of reef fishes. *Mar. Biol.* 164:224. doi: 10.1007/s00227-017-3272-0

Mackensen, A., and Schmiedl, G. (2019). Stable carbon isotopes in paleoceanography: Atmosphere, oceans, and sediments. *Earth Sci. Rev.* 197:102893. doi: 10.1016/j.earscirev.2019.102893

Matley, J. K., Fisk, A. T., Tobin, A. J., Heupel, M. R., and Simpfendorfer, C. A. (2016). Diet-tissue discrimination factors and turnover of carbon and nitrogen stable isotopes in tissues of an adult predatory coral reef fish, Plectropomus leopardus. *Rapid Commun. Mass Spectrom.* 30, 29–44. doi: 10.1002/rcm.7406

Matley, J. K., Tobin, A. J., Simpfendorfer, C. A., Fisk, A. T., and Heupel, M. R. (2017). Trophic niche and spatio-temporal changes in the feeding ecology of two sympatric species of coral trout (Plectropomus leopardus and P. laevis). *Mar. Ecol. Prog. Series* 563, 197–210. doi: 10.3354/meps11971

Mayzaud, P., Chanut, J. P., and Ackman, R. G. (1989). Seasonal changes of the biochemical composition of marine particulate matter with special reference to fatty acids and sterols. *Mar. Ecol. Prog. Series* 56, 189–204. doi: 10.3354/meps056189

McCauley, D. J., DeSalles, P. A., Young, H. S., Papastamatiou, Y. P., Caselle, J. E., Deakos, M. H., et al. (2014). Reliance of mobile species on sensitive habitats: A case study of manta rays (Manta alfredi) and lagoons. *Mar. Biol.* 161, 1987–1998. doi: 10.1007/s00227-014-2478-7

McMahon, K. W., Thorrold, S. R., Houghton, L. A., and Berumen, M. L. (2016). Tracing carbon flow through coral reef food webs using a compound-specific stable isotope approach. *Oecologia* 180, 809–821. doi: 10.1007/s00442-015-3475-3

Ménard, F., Benivary, H. D., Bodin, N., Coffineau, N., Le Loc'h, F., Mison, T., et al. (2014). Stable isotope patterns in micronekton from the Mozambique Channel. *Deep Sea Res. Part II* 100, 153–163. doi: 10.1016/j.dsr2.2013.10.023

Miller, S. D., Zgliczynski, B. J., Fox, M. D., Kaufman, L. S., Michener, R. H., Sandin, S. A., et al. (2019). Niche width expansion of coral reef fishes along a primary production gradient in the remote central Pacific. *Mar. Ecol. Prog. Series* 625, 127–143. doi: 10.3354/meps13023

Miyajima, T., and Umezawa, Y. (2010). "Stable isotope composition of nitrogen (δ^{15}N) as a tool for investigating nitrogen cycling in coral reef ecosystems," in *Earth, Life, and Isotopes*, eds N. Ohkouchi, I. Tayasu, and K. Koba (kyoto: Kyoto University Press), 197–222.

Mock, T., and Gradinger, R. (2000). Changes in photosynthetic carbon allocation in algal assemblages of Arctic sea ice with decreasing nutrient concentrations and irradiance. *Mar. Ecol. Prog. Series* 202, 1–11. doi: 10.3354/meps202001

Morimoto, N., Umezawa, Y., San Diego-McGlone, M. L., Watanabe, A., Siringan, F. P., and Tanaka, Y. (2017). Spatial dietary shift in bivalves from embayment with river discharge and mariculture activities to outer seagrass beds in northwestern Philippines. *Mar. Biol.* 164:84. doi: 10.1007/s00227-016-3063-z

Munday, P. L. (2001). Fitness consequences of habitat use and competition among coral-dwelling fishes. *Oecologia* 128, 585–593. doi: 10.1007/s004420100690

Nakamura, Y., Horinouchi, M., Shibuno, T., Tanaka, Y., Miyajima, T., Koike, I., et al. (2008). Evidence of ontogenetic migration from mangroves to coral reefs by black-tail snapper Lutjanus fulvus: Stable isotope approach. *Mar. Ecol. Prog. Series* 355, 257–266. doi: 10.3354/meps07234

Nakazawa, T. (2015). Ontogenetic niche shifts matter in community ecology: A review and future perspectives. *Popul. Ecol.* 57, 347–354. doi: 10.1007/s10144-014-0448-z

Nash, K. L., Welsh, J. Q., Graham, N. A., and Bellwood, D. R. (2015). Home-range allometry in coral reef fishes: Comparison to other vertebrates, methodological issues and management implications. *Oecologia* 177, 73–83. doi: 10.1007/s00442-014-3152-y

Newell, R. I., and Jordan, S. J. (1983). Preferential ingestion of organic material by the American oyster Crassostrea virginica. *Mar. Ecol. Prog. Series*. 13, 47–53. doi: 10.3354/meps013047

Newman, S. P., Handy, R. D., and Gruber, S. H. (2012). Ontogenetic diet shifts and prey selection in nursery bound lemon sharks, Negaprion brevirostris, indicate a flexible foraging tactic. *Environ. Biol. Fishes* 95, 115–126. doi: 10.1007/s10641-011-9828-9

Oakes, J. M., and Connolly, R. M. (2004). Causes of sulfur isotope variability in the seagrass, Zostera capricorni. *J. Exper. Mar. Biol. Ecol.* 302, 153–164. doi: 10.1016/j.jembe.2003.10.011

O'Farrell, S., Bearhop, S., McGill, R. A. R., Dahlgren, C. P., Brumbaugh, D. R., and Mumby, P. J. (2014). Habitat and body size effects on the isotopic niche space of invasive lionfish and endangered Nassau grouper. *Ecosphere* 5, 1–11. doi: 10.1890/ES14-00126.1

Oksanen, J. F., Blanchet, G., Friendly, M., Kindt, R., Legendre, P., McGlinn, P., et al. (2020). *vegan: Community Ecology Package. R package version 2.5-7.*

Page, H. M., Brooks, A. J., Kulbicki, M., Galzin, R., Miller, R. J., Reed, D. C., et al. (2013). Stable Isotopes Reveal Trophic Relationships and Diet of Consumers in Temperate Kelp Forest and Coral Reef Ecosystems. *Oceanography* 26, 180–189. doi: 10.5670/oceanog.2013.61

Pakhomov, E. A., Henschke, N., Hunt, B. P. V., Stowasser, G., and Cherel, Y. (2019). Utility of salps as a baseline proxy for food web studies. *J. Plankton Res.* 41, 3–11. doi: 10.1093/plankt/fby051

Peterson, B. J. (1999). Stable isotopes as tracers of organic matter input and transfer in benthic food webs: A review. *Acta Oecol.* 20, 479–487. doi: 10.1016/S1146-609X(99)00120-4

Peterson, B. J., and Fry, B. (1987). Stable isotopes in ecosystem studies. *Annu. Rev. Ecol. System.* 18, 293–320. doi: 10.1146/annurev.es.18.110187.001453

Peterson, B. J., Howarth, R. W., and Garritt, R. H. (1986). Sulfur and Carbon Isotopes as Tracers of Salt-Marsh Organic Matter Flow. *Ecology* 67, 865–874. doi: 10.2307/1939809

Pinnegar, J. K., and Polunin, N. V. C. (1999). Differential fractionation of delta C-13 and delta N-15 among fish tissues: Implications for the study of trophic interactions. *Funct. Ecol.* 13, 225–231. doi: 10.1046/j.1365-2435.1999.00301.x

Plass-Johnson, J. G., McQuaid, C. D., and Hill, J. M. (2015). The effects of tissue type and body size on δ^{13}C and δ^{15}N values in parrotfish (Labridae) from Zanzibar, Tanzania. *J. Appl. Ichthyol.* 31, 633–637. doi: 10.1111/jai.12746

Post, D. M., Layman, C. A., Arrington, D. A., Takimoto, G., Quattrochi, J., and Montaña, C. G. (2007). Getting to the fat of the matter: Models, methods and assumptions for dealing with lipids in stable isotope analyses. *Oecologia* 152, 179–189. doi: 10.1007/s00442-006-0630-x

Quaeck-Davies, K., Bendall, V. A., MacKenzie, K. M., Hetherington, S., Newton, J., and Trueman, C. N. (2018). Teleost and elasmobranch eye lenses as a target for life-history stable isotope analyses. *PeerJ* 6:e4883. doi: 10.7717/peerj.4883

R Core Team (2021). *R: A language and environment for statistical computing.* Vienna: R Foundation for Statistical Computing.

R Studio Team (2020). *RStudio: Integrated Development for R.* Boston, MA: RStudio.

Rau, G. H., Sweeney, R. E., and Kaplan, I. R. (1982). Plankton 13C: 12C ratio changes with latitude: Differences between northern and southern oceans. *Deep Sea Res. Part A* 29, 1035–1039. doi: 10.1016/0198-0149(82)90026-7

Richoux, N. B., and Froneman, P. W. (2009). Plankton trophodynamics at the subtropical convergence, Southern Ocean. *J. Plankton Res.* 31, 1059–1073. doi: 10.1093/plankt/fbp054

Riverón, S., Raoult, V., Slip, D. J., and Harcourt, R. G. (2022). Lipid extraction has tissue-dependent effects on isotopic values (δ34S, δ13C, and δ15N) from different marine predators. *Rapid Commun. Mass Spectrom.* 36, e9346. doi: 10.1002/rcm.9346

Roy, A.-S., Frisch, A. J., Syms, C., Thorrold, S. R., and Jones, G. P. (2012). Retention of a transgenerational marker (137Barium) in tissues of adult female anemonefish and assessment of physiological stress. *Environ. Biol. Fishes* 96, 459–466. doi: 10.1007/s10641-012-0029-y

San Diego-McGlone, M. L., Villanoy, C. L., and Aliño, P. M. (1995). Nutrient mediated stress on the marine communities of a coastal lagoon (Puerto Galera, Philippines). *Mar. Pollut. Bull.* 31, 355–366. doi: 10.1016/0025-326X(95)00170-R

Skinner, C., Cobain, M. R. D., Zhu, Y., Wyatt, A. S., and Polunin, N. V. C. (in press). Progress and direction in the use of stable isotopes to understand complex coral reefecosystems: A review. *Oceanogr. Mar. Biol.* 60.

Skinner, C., Newman, S. P., Mill, A. C., Newton, J., and Polunin, N. V. C. (2019b). Prevalence of pelagic dependence among coral reef predators across an atoll seascape. *J. Anim. Ecol.* 88, 1564–1574. doi: 10.1111/1365-2656.13056

Skinner, C., Mill, A. C., Newman, S. P., Newton, J., Cobain, M. R. D., and Polunin, N. V. C. (2019a). Novel tri-isotope ellipsoid approach reveals dietary variation in sympatric predators. *Ecol. Evol.* 9, 13267–13277. doi: 10.1002/ece3.5779

Skinner, M. M., Martin, A. A., and Moore, B. C. (2016). Is lipid correction necessary in the stable isotope analysis of fish tissues? *Rapid Commun. Mass Spectrom.* 30, 881–889. doi: 10.1002/rcm.7480

Søreide, J. E., Tamelander, T., Hop, H., Hobson, K. A., and Johansen, I. (2006). Sample preparation effects on stable C and N isotope values: A comparison of methods in Arctic marine food web studies. *Mar. Ecol. Prog. Series* 328, 17–28. doi: 10.3354/meps328017

Stowasser, G., Atkinson, A., McGill, R. A. R., Phillips, R. A., Collins, M. A., and Pond, D. W. (2012). Food web dynamics in the Scotia Sea in summer: A stable isotope study. *Deep Sea Res. Part II* 59-60, 208–221. doi: 10.1016/j.dsr2.2011.08.004

Sweeting, C. J., Polunin, N. V., and Jennings, S. (2006). Effects of chemical lipid extraction and arithmetic lipid correction on stable isotope ratios of fish tissues. *Rapid Commun. Mass Spectrom.* 20, 595–601. doi: 10.1002/rcm.2347

Thibodeau, B., Miyajima, T., Tayasu, I., Wyatt, A. S. J., Watanabe, A., Morimoto, N., et al. (2013). Heterogeneous dissolved organic nitrogen supply over a coral reef: First evidence from nitrogen stable isotope ratios. *Coral Reefs* 32, 1103–1110. doi: 10.1007/s00338-013-1070-9

Thomas, S. M., and Crowther, T. W. (2015). Predicting rates of isotopic turnover across the animal kingdom: A synthesis of existing data. *J. Anim. Ecol.* 84, 861–870. doi: 10.1111/1365-2656.12326

Tieszen, L. L., Boutton, T. W., Tesdahl, K. G., and Slade, N. A. (1983). Fractionation and turnover of stable carbon isotopes in animal tissues: Implications for $\delta^{13}C$ analysis of diet. *Oecologia* 57, 32–37. doi: 10.1007/BF00379558

Trust, B. A., and Fry, B. (1992). Stable sulphur isotopes in plants: A review. *Plant Cell Environ.* 15, 1105–1110. doi: 10.1111/j.1365-3040.1992.tb01661.x

Vander Zanden, M. J., Clayton, M. K., Moody, E. K., Solomon, C. T., and Weidel, B. C. (2015). Stable isotope turnover and half-life in animal tissues: A literature synthesis. *PLoS One* 10:e0116182. doi: 10.1371/journal.pone.0116182

Wallace, A. A., Hollander, D. J., and Peebles, E. B. (2014). Stable Isotopes in Fish Eye Lenses as Potential Recorders of Trophic and Geographic History. *PLoS One* 9:e108935. doi: 10.1371/journal.pone.0108935

Wang, B., and LinHo. (2002). Rainy Season of the Asian–Pacific Summer Monsoon. *J. Climate* 15, 386–398. doi: 10.1175/1520-0442(2002)015<0386:RSOTAP>2.0.CO;2

Wantzen, K. M., de Arruda Machado, F., Voss, M., Boriss, H., and Junk, W. J. (2002). Seasonal isotopic shifts in fish of the Pantanal wetland, Brazil. *Aqua. Sci.* 64, 239–251. doi: 10.1007/PL00013196

World Weather Online (2022). *Puerto Galera Historical Weather*.Manchester: World Weather Online.

Wyatt, A. S. J., Falter, J. L., Lowe, R. J., Humphries, S., and Waite, A. M. (2012a). Oceanographic forcing of nutrient uptake and release over a fringing coral reef. *Limnol. Oceanogr.* 57, 401–419. doi: 10.4319/lo.2012.57.2.0401

Wyatt, A. S. J., Waite, A. M., and Humphries, S. (2012b). Stable isotope analysis reveals community-level variation in fish trophodynamics across a fringing coral reef. *Coral Reefs* 31, 1029–1044. doi: 10.1007/s00338-012-0923-y

Wyatt, A. S. J., Lowe, R. J., Humphries, S., and Waite, A. M. (2013). Particulate nutrient fluxes over a fringing coral reef: Source-sink dynamics inferred from carbon to nitrogen ratios and stable isotopes. *Limnol. Oceanogr.* 58, 409–427. doi: 10.4319/lo.2013.58.1.0409

Wyatt, A. S. J., Matsumoto, R., Chikaraishi, Y., Miyairi, Y., Yokoyama, Y., Sato, K., et al. (2019). Enhancing insights into foraging specialization in the world's largest fish using a multi-tissue, multi-isotope approach. *Ecol. Monogr.* 89:e01339. doi: 10.1002/ecm.1339

Zgliczynski, B. J., Williams, G. J., Hamilton, S. L., Cordner, E. G., Fox, M. D., Eynaud, Y., et al. (2019). Foraging consistency of coral reef fishes across environmental gradients in the central Pacific. *Oecologia* 191, 433–445. doi: 10.1007/s00442-019-04496-9

Zhu, Y., Newman, S. P., Reid, W. D. K., and Polunin, N. V. C. (2019). Fish stable isotope community structure of a Bahamian coral reef. *Mar. Biol.* 166:160. doi: 10.1007/s00227-019-3599-9

Zikova, A. V., Britaev, T. A., Ivanenko, V. N., and Mikheev, V. N. (2011). Planktonic and symbiotic organisms in nutrition of coralobiont fish. *J. Ichthyol.* 51, 769–775. doi: 10.1134/S0032945211060105